universität wien

MASTERARBEIT | MASTER'S THESIS

Titel | Title

Towards Sustainable Pesticides: Extraction of Orange Peel Flavonoids and Their Soil Biotransformation

verfasst von | submitted by

Alban Beaujean BSc

angestrebter akademischer Grad | in partial fulfilment of the requirements for the degree of

Master of Science (MSc)

Wien | Vienna, 2025

Studienkennzahl lt. Studienblatt | Degree programme code as it appears on the student record sheet:	UA 066 299
Studienrichtung lt. Studienblatt | Degree programme as it appears on the student record sheet:	Masterstudium Environmental Systems: Processes - Pollution - Solutions
Betreut von | Supervisor:	Assoz. Prof. Dr. Michael Zumstein

Acknowledgement

First, I would like to thank my supervisor, Assoc.-Prof. Dr. Michael Zumstein. I've rarely experienced such interest and consistent engagement in supervised students – which, all the more, motivated me to give my best. Thank you for the opportunity to be part of the research group and for the constructive guidance during our meetings.

I'd like to especially thank my mentor Richard Gruseck. Being able to knock on your door with questions at any time – and feeling genuinely welcome to do so – as well as your profound understanding of your field made a big difference in how much I was able to learn during this work.

Finally, to the entire lab team at EDGE: thank you for the open, collaborative atmosphere and for all the support throughout this project.

Abstract

Flavonoids have antibacterial and fungicidal properties and are therefore considered promising candidates for use as biopesticides. While the relationship between flavonoid structure and their biotransformation in soils – an important aspect for sustainable pesticides – has recently been investigated for individual flavonoids, it remains unclear to what extent findings of such studies are transferrable to flavonoids extracted together with co-extracted compounds in natural extracts. In this study, we addressed such an application-oriented scenario and extracted from orange peels using ethanol and a deep eutectic solvent (choline chloride/urea). We assessed the feasibility of sourcing flavonoids from natural waste, by evaluating extraction yields and composition variability across different batches. Therefore, extraction protocols were optimized, and extracts from four different batches were analyzed for total phenolic content (TPC) using UV-Vis spectroscopy and for individual flavonoids using HPLC-HRMS. While flavonoids accounted for approximately 40 % of the TPC, substantial variation in this ratio between batches limited the usefulness of TPC as a consistent proxy. Average total flavonoid yields across four commercial orange batches were approximately 1.2–1.3 % of dry weight for extractions with both solvents. The dominant constituents were hesperidin, naringin, and fully methoxylated flavones (4–7 OMe). The relatively consistent extraction yields suggest commercial oranges may offer a stable flavonoid source for biopesticide development. Soil biodegradation studies of the full extracts revealed complete transformation of glycosylated flavonoids within two days, whereas the fully methoxylated flavones exhibited slower transformation (maximum 50 % during three weeks). The observed transformation rates were considerably slower than those reported for pure flavonoids, likely due to mixture effects from co-extracted substances. In addition, the position rather than the number of OMe appeared to govern PMF stability. These findings highlight the relevance of a holistic, matrix-aware perspective when evaluating the biotransformation and environmental fate of biopesticides.

Kurzfassung

Flavonoide haben antibakterielle und fungizide Eigenschaften, weshalb sie zunehmend als vielversprechende Kandidaten für den Einsatz als Biopestizide gelten. Während der Zusammenhang zwischen Flavonoid-Struktur und dessen Abbauverhalten – ein entscheidender Aspekt für nachhaltige Pestizide – von reinen Flavonoiden in Böden zuletzt untersucht wurde, ist unklar, inwieweit sich diese Erkenntnisse auf Gemische mit co-extrahierten Stoffen aus natürlichen Extrakten übertragen lassen. In dieser Arbeit wurde ein praxisnäheres Szenario untersucht, bei dem Flavonoide aus Orangenschalen mithilfe von Ethanol und einem Deep Eutectic Solvent (Cholinchlorid/Urea) extrahiert wurden. Zur Bewertung der Eignung natürlicher Abfallprodukte für die Flavonoidgewinnung wurden Extraktionsausbeuten und die Zusammensetzung verschiedener Chargen analysiert. Dafür wurden Extraktionsprotokolle optimiert und Extrakte aus vier verschiedenen Chargen auf den Gesamtphenolgehalt (TPC) mittels UV-Vis-Spektroskopie sowie auf einzelne Flavonoide mittels HPLC-HRMS analysiert. Obwohl Flavonoide im Schnitt rund 40 % des TPC ausmachten, schränkte die zwischen den Chargen beobachtete Variabilität die Eignung des TPC als verlässlichen Proxy ein. Die durchschnittlichen Gesamtflavonoid-Ausbeuten über vier handelsübliche Orangenchargen lagen bei etwa 1,2–1,3 % des Trockengewichts für Extraktionen mit beiden Lösungsmitteln, wobei vorwiegend Hesperidin, Naringin und voll methoxylierte Flavone (PMFs) (mit 4–7 Methoxygruppen) gefunden wurden. Die vergleichsweise konstanten Ausbeuten sprechen dafür, dass handelsübliche Orangen eine stabile Quelle für Flavonoide zur Entwicklung von Biopestiziden sein könnten. Abbaustudien der gesamten Extrakte in Bodenproben zeigten eine vollständige Umwandlung der glycosylierten Flavonoide innerhalb von zwei Tagen, während PMFs über drei Wochen eine langsamere Transformation von maximal 50% aufwiesen. Die beobachteten Abbauraten waren deutlich langsamer als die für die reinen, einzelnen Flavonoide berichteten, was wahrscheinlich auf Auswirkungen mitextrahierter Substanzen zurückzuführen ist. Außerdem scheint mehr die Position der Methoxygruppen als deren Anzahl die Stabilität der PMFs zu bestimmen. Diese Ergebnisse verdeutlichen, wie wichtig eine ganzheitliche, matrixbezogene Perspektive für die Beurteilung des Abbauverhaltens bio-basierter Pestizide ist.

Contents

List of Figures

List of Tables

List of Abbreviations

ChCl/U20	Choline chloride/urea (1:2 molar ratio, 20% water content)
DW	Dry weight
EtOH60	ethanol/water 60:40 v/v
GAE	Gallic acid equivalents
UHPLC-HRMS	Ultra-High Performance Liquid Chromatography coupled to High Resolution Mass Spectrometry
OMe	methoxy groups
PMFs	Polymethoxylated flavonoids
RSD	Relative standard deviation
S/L ratio	Solid-to-liquid ratio
TPC	Total phenolic content

Introduction

Worldwide, pesticide use is on the rise. Between 1990 and 2021, the amount of pesticides used in agriculture doubled to 3.5 million tons of active ingredients[1]. This trend is expected to continue, with climate change further driving the global rise in the quantity of pesticide use[2]. The environmental footprint of this extensive use is already clearly measurable. Pesticide residues were found in over 80% of 317 soil samples from across the European Union[3], revealing their widespread application and persistence. The slow degradation of these substances is also evident in agricultural fields, where former applied pesticides remain detectable for up to two decades and have been linked to reduced microbial biomass and impaired beneficial fungi[4]. These residues are not only persistent in the environment but have also been linked to a range of environmental consequences, including ground- and drinking water contamination[5–7]. In soil, pesticide residues disrupt microbial processes like nitrogen cycling and reduce microbial diversity, contributing to soil degradation[4,8,9]. Due to their mobility they often impact areas beyond their original site of use[4,10]. To reduce the detrimental effects on the environment caused by synthetic pesticides, a shift toward the broader use of biopesticides could represent a promising alternative. Biopesticides are intended to be biodegradable, plant- or microbe-derived and act in more targeted ways, rather than through unspecific chemical toxicity, meeting key criteria for safer human and environmental health[11].

Due to this demand for more sustainable pesticides, flavonoids have gained increasing attention[12]. Flavonoids are polyphenols – a group of secondary plant metabolites found in many plants[13]. Among other roles, they act as intrinsic defense agents against biotic stressors, supporting both direct defense and indirect mechanisms such as protective barriers[14,15]. Several studies have reported antibacterial, fungicidal, and potentially insecticidal properties of flavonoids like hesperidin, naringin, and different PMFs[16–18]. For instance, the combination of PMFs and citral demonstrated strong antifungal activity by damaging the cell membrane against P. digitatum, a mold fungus that infects post-harvest citrus fruits and causes significant crop losses[17].

One promising source of flavonoids is orange peel. In 2023 approximately 70 million tons of oranges were produced globally19, of which an estimated 50-60% typically ends up as organic waste20. Two key flavonoid subclasses in citrus fruits – flavones and flavanones – are especially abundant. Flavanones mainly occur in glycosylated forms such as hesperidin and naringin, while flavones are commonly present as PMFs often containing four or more OMe21,22. As an agricultural waste product, orange peels represent a rich flavonoid source that is both cost-effective and available in large quantities. The chemical structures of the two major glycosylated flavanones, their corresponding aglycones, and representative fully methoxylated PMFs with four to seven OMe are shown in **Table 1**.

Table 1: *Chemical structures of key flavonoids found in orange peel: glycosylated flavanones (hesperidin, naringin), their aglycones (hesperetin, naringenin), and representative fully methoxylated PMFs containing 4–7 OMe. Structures were drawn using MolView*[23].

Compound	Flavonoid type	structure
Naringin	Flavanone	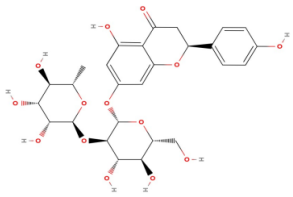
Naringenin	Flavanone	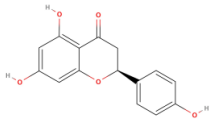
Hesperidin	Flavanone	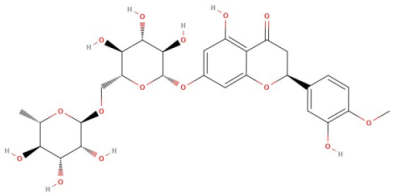
Hesperetin	Flavanone	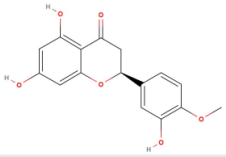
PMF with 4 methoxy groups (example)	Flavone	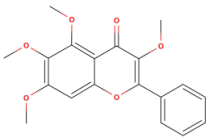
PMF with 5 methoxy groups (example)	Flavone	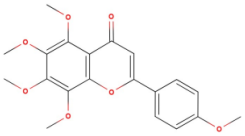
PMF with 6 methoxy groups (example)	Flavone	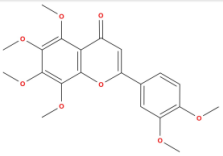
PMF with 7 methoxy groups (example)	Flavone	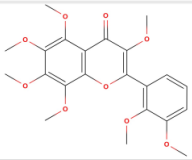

For the extraction of these flavonoids from matrices such as orange peels, deep eutectic solvents have emerged as promising alternatives to conventional organic solvents[24]. Described by Abbott et al. in 2003 as the first DES[25], ChCl:urea (1:2) laid the basis for the development of a broad range of DES combinations, now classified into four main types. While flavonoids have already been extracted from different plants using a wide variety of DESs[26–28], ChCl:urea (1:2) still remains one of the most commonly used DES[29]. It is frequently described as readily biodegradable and practically harmless for aquatic organisms such as fish and crustaceans, though it shows moderate toxicity in mice[30]. In contrast, other DESs can show inconsistent biodegradability[31,32] and may be more toxic than their individual components[24,30]. These observations suggest that, while DESs offer the potential for more sustainable solvents, their actual environmental impact strongly depends on their specific composition. Therefore, ChCl:urea was chosen in this study, as the 1:2 ratio is considered relatively safe and has been shown to be readily biodegradable.

DESs are typically composed of a hydrogen bond donor and a hydrogen bond acceptor. To illustrate the functionality and advantages of these solvents, the DES used in this is discussed in more detail below. The chloride anion forms strong hydrogen bonds with the hydrogen atoms of the amino groups in urea, as well as with the hydroxyl group of the choline cation. These interactions result in a significant depression of the melting points of the individual components, leading to the formation of a liquid eutectic mixture at room temperature. The resulting solvent is characterized by a high polarity and the ability to form extensive hydrogen-bonding networks.[29,33,34]

Numerous studies have focused on optimizing the extraction efficiency of phenolic compounds and flavonoids from orange peel using both DES and conventional organic solvents[35–41]. Due to its relatively fast determination via spectrophotometric methods, TPC is useful and can serve as an approximate indicator for estimating total flavonoid yield in orange extracts, although it does not allow for the identification or quantification of individual flavonoid compounds. Few studies have actually measured both TPC and flavonoid content using UHPLC-HRMS to directly compare their correlation[37,38], with other studies focusing solely on flavonoid content[39–41].

When comparing the reported yields of TPC and individual flavonoids in orange peel extracts, the scientific literature presents a highly inconsistent picture. While some studies report relatively low TPC values – ranging from 0.6 - 4 mg GAE/g DW[36,38,42] – others achieve significantly higher yields, exceeding 30 mg GAE/g DW[37]. Similar discrepancies can be observed for the exact determination of individual flavonoids such as hesperidin, naringin, or PMFs using UHPLC-HRMS, with concentrations for e.g. hesperidin ranging from 0.18 mg/g DW[39] up to very high yields like 35.38 mg/g DW using methanol[40] and 47 mg/g DW using DES[41]. However, these differences cannot be explained by using either DES or organic solvents, as comparable yields have been observed for both solvents within the same study. Previous studies are lacking consistency regarding key parameters that could explain these variations. Different orange varieties are used, while rarely specifying the exact cultivar or whether the fruit was organically or conventionally grown. Furthermore, details on the batches, harvest time, or storage conditions are frequently missing. Extraction procedures also vary widely in terms of S/L ratio, size of the powder – ranging from < 0,177mm[41] to > 1cm[40], duration and circumstances of powder storage, further complicating direct comparisons. This variability is exemplified by one study that stored orange peel powder at room temperature for several months before extraction[39], despite evidence from another showing that cold storage of whole fruits for just three months can significantly lower hesperidin content[38]. As a result, it remains unclear whether orange peel waste in general can be considered a viable and reproducible source for efficient flavonoid extraction.

Aside from achieving efficient and sustainable extraction of flavonoids, understanding their degradation behavior in soil is crucial to avoid long-term environmental impacts. This has been scarcely studied to date. Flavonoids introduced into soil via clover intercropping were found to degrade rapidly, with glycosylated compounds breaking down within 1-3 days and forming aglycones as intermediates[43]. Reported degradation times for 90 % of aglycones and their transformation products, such as biochanin A, dihydrobiochanin A, pratensein, and genistein, range from approximately 6 to 15 days[44]. Microbial activity appears to be the primary driver of degradation, while sorption-desorption dynamics may also influence the observed behavior in soil[45].

Building upon these few studies, a more recent investigation represents the first systematic attempt to assess the biotransformation behavior of a broad set of structurally diverse and chemically pure flavonoids relevant for pesticidal application[46]. The study included various aglycones, their glycosylated forms, and – uniquely – methoxylated derivatives, and tested their transformation across different soil types. Core structures such as naringenin, apigenin, and genistein showed half-lives of 2.9 to 12 hours in all tested soils. The methoxylated forms persisted significantly longer. Among these, PMFs with one OMe showed significantly shorter half-lives of maximum three days, than those substituted with three OMe, which showed half-lives of more than 18 days. In contrast, glycosylated flavonoids were transformed rapidly into their aglycones, with half-lives of 1 to 5 hours, indicating substantial variability in transformation kinetics depending on structural features. While this study provides important insights into the transformation of individual flavonoids added to the soil in pure form, in practical applications, crude extracts containing various co-extracted compounds would be applied. The presence of these additional compounds like other phenols may significantly alter the transformation behavior, as they can alter soil microbial activity[47,48] resulting in slower or even faster transformation patterns. This highlights the need for a more comprehensive understanding of flavonoid mixtures in real-world conditions.

The overview of existing studies on flavonoid extraction and transformation reveals clear research gaps. On the one hand, it remains unclear whether large fluctuations in flavonoid yields from orange peel are mainly caused by non-standardized extraction procedures or by natural variations in the raw material. On the other hand, it is not yet known to what extent transformation kinetics determined for pure flavonoids in soil apply to flavonoids extracted from orange peel, which occur as complex mixtures with co-extracted compounds. Therefore, this study focuses on a standardized extraction of flavonoids from peels from different orange batches, using the previously applied DES ChCl:urea (1:2) as a more sustainable alternative to conventional organic solvents, and aims to provide pesticidal-relevant insights into the transformation pathways of these flavonoid-rich extracts in soil.

Firstly, due to the considerable variability in reported TPC values in the literature, the extraction method is re-evaluated using a total phenolic assay. A DES-based approach is employed, as these are considered a more sustainable alternative to conventional solvents. This

part focuses on optimizing key extraction parameters, including a renewed investigation of different S/L ratios and two distinct particle sizes of the orange peel powder. Additionally, the storage stability of the dried material is assessed. This provides the experimental foundation necessary to reliably test the hypotheses of the following two parts.

Secondly, we applied the optimized extraction method to investigate both intra- and inter-batch variability among different orange batches, including organic and conventional oranges, as well as fruits from different countries. To test whether natural variation allows certain batches to serve as a better source for pesticide production, we analyzed TPC values alongside UHPLC-HRMS data on individual flavonoids and their relative abundances.

Finally, the orange peel extract is applied to soil samples. The biotransformation kinetics of the extracted glycosylated and polymethoxylated flavonoids are monitored over a period of three weeks in both active and autoclaved soils to investigate how the presence of co-extracted compounds influences their transformation compared to isolated, pure flavonoids.

Materials and Methods

Chemicals and Materials

The following chemicals were purchased from Sigma Aldrich: choline chloride (purity: ≥98%, C1879-500G), gallic acid monohydrate (purity: ≥99%, 27645-250G-R), Sodium carbonate (Na_2CO_3, purity: ≥ 99.5%, 222321-500g) and Folin & Ciocalteu's phenol reagent (47641-100ML-F). In addition, citric acid (purity: ≥99%, Merck, K91297207 615), urea (CAS: 57-13-6, Fisher Scientific, U/0500/53) and ethanol (CAS: 64-17-5, Acros Organics, 181970010) were used.

Chemical reference standards of hesperidin (≥95%, AB353767), catechin ((+)-catechin hydrate, 95%, AB139275), kaempferol (95%, AB148852), luteolin (97%, AB151922), naringenin ((±)-naringenin, ≥95%, N5893), genistein (96%, AB136269), apigenin (95%, AB402813), rutin (quercetin-glc-rha, 95%, AB401423), naringin (naringenin-glc-rha, ≥95%, 71162), quercetin (95%, AB171856), myricetin (97%, AB353731), diosmetin/chrysoeriol (4'-methylluteolin, 98%, AB253844 / 3'-methylluteolin, 99%, AB253903), TetraMetLuteolin (3',4',5,7-tetramethoxyflavone, 97%, AB179893), TriMetApigeninNew (5,7,4'-trimethoxyflavone, AB151972), kaempferol-glc (kaempferol-3-O-glucoside, 99%, AB148850), apigenin-glc (apigenin-7-O-glucoside, AB253874), and genkwanin (7-methoxyapigenin, 97%, AB179829) were obtained from Sigma-Aldrich, while hesperetin was purchased from cayman chemical company (Item: 10006084, Batch: 0610850-5).

Centrifuge tubes with volumes of 15 mL (525-0629) and 50 mL (525-0631) were sourced from VWR, while 2 mL Safe-Lock tubes (0030120094) were obtained from Eppendorf. Solvents including acetonitrile (HPLC gradient grade, ≥99.9%, A/0627/17), methanol (HPLC grade, ≥99.8%, M/4056/17), acetone (extra pure, 10244202), and formic acid (LC/MS grade, ≥99.0%, 10596814) were purchased from Fisher Scientific. In addition, hypergrade methanol for LC-MS (1.06035.2500) was obtained from Merck.

All solutions were prepared with ultra-pure water using a PURELAB Chorus system (0.071 µS/cm, Elga Veolia). All chemicals and solvents were of analytical grade and used without further purification unless stated otherwise.

Orange Peel Processing

Fresh oranges were sourced from different suppliers and origins (see **Table SI 2**) and processed on the same day of purchasing. The batches included organic and conventional oranges from South Africa, Greece, Botswana, Italy, and one unknown origin.

Oranges were peeled leaving a small amount of white pith on the fruit (see **Figure SI 1**). For two separate batches (each consisting of three oranges), both the weight of the whole fruit and the corresponding fresh and dried peel were recorded (see **Table SI 3**). For the remaining oranges, only the peel was collected and processed into powder without prior weighing. After peeling, the collected orange peels were dried at 60°C for approximately 6.5 hours until a constant weight was achieved in two consecutive measurements. The dried peel was ground three times for 30 seconds each, with breaks between grinding steps to prevent overheating, using a KYG mini grinder (Model No. LH711). The resulting powder was sieved through a 355 µm sieve. The sieved powder was stored in the dark in Schott bottles at room temperature for a maximum of 4 weeks.

Extractions

The DES was mixed using choline chloride and urea in a 1:2 molar ratio with 20% water content[34]. Based on the density reported by Zhao et al.[34], the required amount of water was calculated and added at the beginning of the preparation to facilitate mixing due to the relatively high viscosity of the DES. The mixture was gently stirred at 50°C for around 30 minutes until a transparent and homogeneous solution was obtained. The final DES was stored at room temperature in Schott bottles.

For extraction, powdered peel was transferred to 2 mL Eppendorf tubes, and either ChCl/U20 or EtOH60 was added to achieve an S/L ratio of 1:5, 1:10, or 1:25. The mixture was vortexed until fully suspended and incubated at 50°C for 30 minutes in a shaker (Eppendorf ThermoMixer F2.0, Cat. No. 5387000013) at 1000 rpm. All extractions were performed in triplicates. Following extraction, samples were centrifuged at 20,800 g for 30 minutes. The supernatant was diluted 1:10 with water and centrifuged again at 20,800 g for 2 minutes. Subsequently, one portion of the supernatant was frozen for later analysis with UHPLC-

HRMS, while another portion was further diluted to a final 1:100 dilution prior to TPC measurement. Prior to UHPLC-HRMS measurements, samples were thawed, vortexed, and further diluted to a final 250-fold dilution in aqueous ethanol (60% (v/v)) before being transferred to vials.

For soil incubations, a larger quantity of extract was required. Therefore, the extraction process was upscaled. Orange peel powder (10 g) was extracted using 100 mL of EtOH60, maintaining an S/L ratio of 1:10. The mixture was magnetically stirred at 50°C and 1000 rpm for 40 minutes. Following extraction, the suspension was transferred into two 50 mL centrifuge tubes and centrifuged at 14,000 g for 30 minutes. The supernatant was divided into 48 × 2 mL Eppendorf tubes, each filled with 1.5 mL. The samples were concentrated at 45°C under vacuum using a SpeedVac system for 3 hours (60 minutes with V-AL and 120 minutes with V-AQ settings).

The viscous concentrate was resolubilized by adding 125 µL of 70% acetonitrile to each tube, resulting in a 12-fold concentration of the original extract. The samples were vortexed thoroughly and stored at -18 °C. Before further use, samples were thawed and homogenized using a spatula, as vortexing alone was insufficient for complete redissolution. For consistency across degradation experiments, all samples were combined with a pipette into a single 10 mL tube. The 12-fold concentration resulted in similar PMF levels to Gruseck et al.[46], ensuring adequate amounts for subsequent degradation experiments.

TPC Measurements

TPC was determined using the Folin-Ciocalteu microassay, following the method of Dabetic et al.[49]. Serial standard solutions of gallic acid (0.05–1.0 mg/mL) were prepared in water. For the assay, 10 µL of 100-fold diluted peel extract, gallic acid standard, or water (blank) was added to a 96-well microplate. Subsequently, 80 µL of 1 M Na_2CO_3 solution and 100 µL of 10-fold diluted Folin-Ciocalteu reagent were added to each well. The plate was incubated in the dark at room temperature for 60 minutes. Absorbance was measured at 630 nm using a Tecan Infinite 200 Pro UV-Vis spectrophotometer (Firmware: V_5.31_04/18_InfiniteRX) with a bandwidth of 9 nm. The measurement was performed after linear shaking (3 s, 1 mm amplitude), and blank wells were used for baseline correction. A linear calibration curve of

gallic acid was constructed by plotting absorbance against concentration with an R^2 value of at least 0.98. The TPC of the extracts was calculated using the equation derived from this curve and expressed as milligrams of gallic acid equivalents per gram of dry weight (mg GAE/g DW) or per milliliter (mg GAE/mL).

Degradation Experiment

5M soil from „Landwirtschaftliche Untersuchungs- und Forschungsanstalt" (LUFA) Speyer was prewetted to 52.3% of its maximum water holding capacity and equilibrated for four days prior to the start of the incubation experiments. To prepare sterile controls, half of the prewetted soil was autoclaved at 121°C for 30 minutes using a Sanoclav LaM-3-20-MCS-J autoclave.

For each time point, triplicate samples were prepared. Prior to application, the extracted and concentrated flavonoid stock solution was vortexed to ensure homogeneity, as the concentrated extract consistently showed rapid phase separation into two approximately equal layers. The upper layer appeared dark yellow and transparent, while the lower layer was light yellow and turbid (see **Figure SI 5**). A total of 10 µL of the stock solution was first applied to approximately one-quarter of the total soil sample (1.18g of soil DW) in a 50 mL centrifuge tube to minimize the impact of acetone on the entire soil microbiome. The soil was briefly mixed, and the acetone solvent was allowed to evaporate for 15 minutes. Subsequently, the remaining soil was added and thoroughly mixed, resulting in a total of 4.7g of soil DW per sample. To determine the initial concentration (T_0), flavonoid solutions were spiked into the full soil matrix and extracted immediately. During incubation, samples were kept at room temperature (~20°C) in the dark. To prevent anoxic conditions, tubes were opened twice per week for one hour. Evaporative water loss during aeration was compensated by individual rehydration (see **Table SI 4** and **Table SI 5**).

To extract flavonoids from soil, a protocol from Andersen et al. was used[50]. First, 10 mL of acetonitrile was added to the soil sample, vortexed, and then agitated at 150 rpm on a horizontal shaker (Universal Shaker SM-30-B, Edmund Bühler GmbH) for 30 minutes. The suspension was centrifuged at 7000 g for 5 minutes, and 5 mL of the supernatant was transferred into a 10 mL centrifuge tube, while the remaining liquid was discarded. In the second extraction step,

the same procedure was repeated using aqueous methanol (70% (v/v)) instead of acetonitrile. The resulting extracts from both steps were combined and stored at -18 °C.

Before analysis, a 1.6 mL aliquot of the extracted flavonoids was transferred into a 2 mL tube and concentrated in a vacuum concentrator (Eppendorf Concentrator plus) at 45°C for 3.5 hours. The resulting dry residue was reconstituted in 800 µL of aqueous methanol (30% v/v)) containing 0.1% formic acid, and thoroughly vortexed and stored at -18 °C until measurement. After thawing, the samples were centrifuged at 20,000 g for 2 minutes, 500 µL of the clarified extract was transferred into UHPLC-HRMS and directly measured.

Analysis of PMFs and Glycosylated Flavonoids by UHPLC-HRMS

Samples were measured by Richard Gruseck according to Gruseck et al.[46]. In Brief: Flavonoids were analyzed using a high-performance liquid chromatography (Vanquish Horizon UHPLC System, Thermo Fisher) coupled to a high-resolution mass spectrometer (HRMS) (Orbitrap Exploris 240, Thermo Fisher). A Phenyl-Hexyl column was used (Acquity Premier CSH, 1.7µm, 2.1 x 100 mm, Waters, article number: 186009478), with an injection volume of 10 µL, a flow rate of 0.4 mL/min, a column compartment temperature of 40°C, and the following eluents: (A) water with 0.1% (v/v) formic acid and (B) methanol with 0.1% (v/v) formic acid. The eluent gradient was as follows: 0-3 min: 20% B, 3-16 min: 20-95% B, 16-18.5 min: 95% B, 18.5-19 min: 95-20% B, 19-22 min: 20% B. The MS parameters were set as follows: ion source: heated electrospray ionization, sheath gas: 50, aux gas: 10, sweep gas: 1, Ion transfer tube temperature: 320°C, vaporizer temperature: 350°C, spray voltage: +3500 V and -2500 V, EASY-IC: start of the run. MS full-scan: range: 100-650 m/z, 3-10 min: 120000 (negative) / 45000 (positive), 10-20 min: 45000 (negative) / 120000 (positive), AGC target: Standard, Maximum IT: AUTO. MS2 spectra were acquired separately with the following settings: MS full-scan: range: 100-650 m/z, 60000 (polarity switching), MS/MS acquisitions: Top 4, resolution 15000, AGC target: 50000, Maximum IT: AUTO, isolation window: 1.0 m/z, NCE: 35, 55, 70 (negative mode) 30, 50, 70 (positive mode).

HRMS data were processed using Skyline software (v22.2.0.527). Flavonoid-aglycones and their glycosylated and methoxylated derivatives were screened, based on the availability of analytical standards (see **Table SI 6**). Naringin was quantified using its own analytical standard (see **Figure SI 2** and **Figure SI 6**). Since no hesperidin standard was available during the experimental phase, hesperidin was quantified using the calibration curve of naringin. After the experiments, a comparison of calibration curves showed that hesperidin produced a significantly lower peak area at the same concentration. Based on this, a correction factor of 2.21 was applied to account for the lower detector response of hesperidin. This correction factor was applied retrospectively to all relevant samples (see **Figure SI 3**). PMFs were identified through targeted screening based on exact mass values reported by Zhang et al.[51] considering exact mass accuracy (±3 ppm) (see **Table SI 7**). Retention times were recorded but not used for identification, as no standards were available for comparison. Quantification of all detected PMFs was carried out using a calibration curve derived from the two available PMF standards, 4′,5,7-trimethoxyflavone and 3′,4′,5,7-tetramethoxyflavone (see **Figure SI 4** and **Figure SI *7***), despite differences in molecular structure and exact mass.

Data processing and analysis were performed in R (v4.3.1) and Microsoft Excel for Microsoft 365 (v2505, Build 16.0.18827.20102, 32-bit). Calibration curves covered a concentration range from 50 nM to 2000 nM. A linear regression model was applied for glycosylated flavonoids, while a quadratic regression model was used for PMFs. Peaks with intensities below 10^6 or retention times exceeding 1 minute were excluded from analysis, ensuring a focus on the major flavonoids rather than trace-level compounds. The limit of quantification (LOQ) was defined as the lowest concentration in the calibration range (50 nM). All flavonoid concentrations were subsequently converted and expressed as mg/g DW. Instrument stability was monitored by performing repeated injections of a single calibration solution throughout the measurement sequence (see **Figure SI *8***).

In addition to quantification via MS1, MS2 spectra were considered to confirm compound identities. For PMFs, characteristic fragment losses in steps of –15 m/z were observed, corresponding to the loss of one or more OMe, with –30 m/z being the most frequently observed. These fragmentation patterns served as diagnostic markers for the presence of

PMFs[52]. In the case of glycosylated flavonoids, the appearance of the respective aglycone fragments in the MS2 spectrum was used to verify the identity of the glycosylated precursor compound.

Results and Discussion

Optimizing Phenolic Extraction

Due to the high variability in extraction yields reported in the literature, the first part of this study aimed to re-evaluate and optimize the extraction of flavonoids from orange peels. This was done using ChCl/U20 in comparison with EtOH60. To address inconsistencies across studies, the S/L ratio, powder particle size, and the stability of TPC over four weeks were re-tested. Other parameters, such as extraction time and temperature, were adopted when they were widely used in literature[24,35,41,53]. For this optimization part TPC was used as a proxy to estimate overall flavonoid yield. While TPC does not provide compound-specific information, it offers a rapid method for screening and comparing all phenolic compounds. This part provided a robust foundation for the subsequent identification and quantification of individual flavonoids using UHPLC-HRMS.

Best Yield-to-Solvent Efficiency Observed at 1:10 S/L Ratio

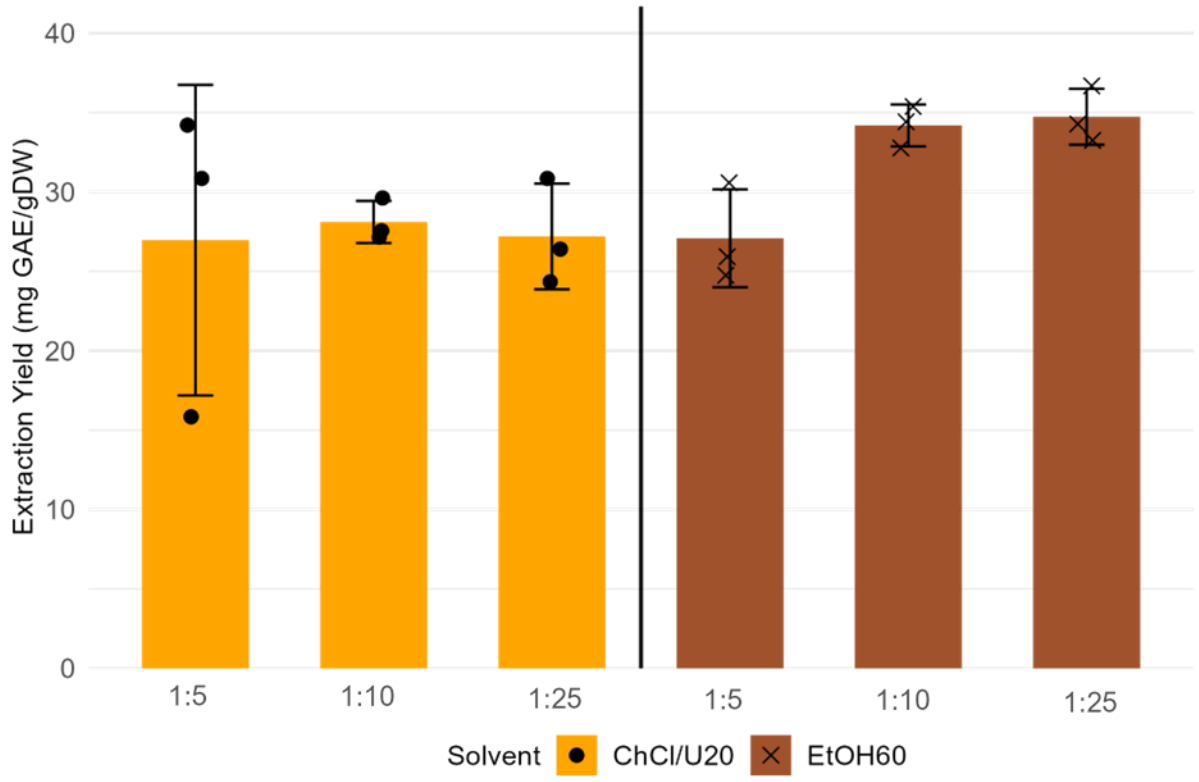

Figure 1: *TPC (mg GAE/g DW) extracted from batch O.NA (see* ***Table SI 2****) at different S/L ratio (1:5, 1:10, and 1:25) using ChCl/U20 and EtOH60. Bars represent the mean values ± standard deviation from three independent extractions.*

To optimize the S/L ratio, the frequently used ratio of 1:10[36,41] was compared with 1:25, representing intermediate ratios reported in the literature[37,41], and 1:5, which was experimentally tested for its potential to achieve higher extraction yields with less solvent. Using ChCl/U20 the results showed no significant difference in yields across all three ratios, with a mean of 27.4 ± 0.6 mg GAE/g DW (see **Figure 1**). The extractions using EtOH60 yielded an average of 32.0 mg ± 4.3 mg GAE/g DW, with 1:5 yielding less than the other two ratios.

As no additional yield could be obtained with a greater proportion of solvent than 1:10 in both cases, an S/L ratio of 1:25 was considered unsuitable. 1:5 showed high variability for ChCl/U20 and lower yields with slightly increased standard deviation for EtOH60, making it also less suitable. Regardless of the solvent used, samples extracted at an S/L ratio of 1:5 were

prone to contamination of the supernatant. This was likely due to the limited volume of the supernatant, which increased the risk of drawing in solid residues during the process of pipetting, which then potentially caused outliers in the UV-Vis measurements. The still higher consistency of ethanol extractions at 1:5 may be due to its lower viscosity compared to DES. After centrifugation, the ChCl/U20 samples did not separate perfectly, which made handling more difficult. Considering all findings, we selected an S/L ratio of 1:10 as the standard method for extraction.

Improved Extraction Efficiency with ≤ 355 µm Particle Size

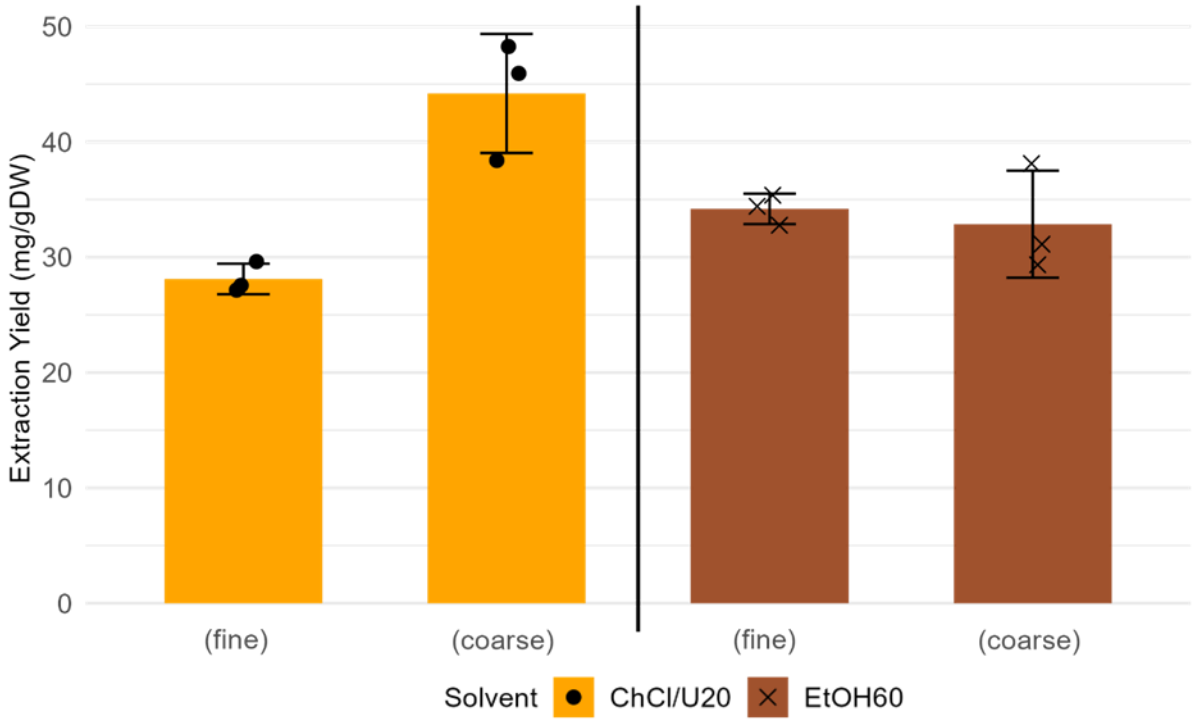

Figure 2: *TPC (mg/gDW) extracted from batch O.NA (see* ***Table SI 2****) with different powder particle sizes (fine: ≤ 250 µm and course: 250 µm < X ≤ 355 µm) using ChCl/U20 and EtOH60 with an S/L ratio of 1:10. Bars represent the mean values ± standard deviation from three independent extractions.*

In previous studies, different particle sizes, ranging from 30-850 µm[35], to 320 µm[41], to 1 mm[36], to 0.5-2.5 cm[53], have been used. Smaller particles have an increased surface area, which can enhance mass transfer. Therefore, we compared the yields achieved with the respective particle

sizes and chose two fractions for our study: fine (≤ 250 µm) and coarse (250 µm < X ≤ 355 µm), primarily based on the findings of Xu et al.[41].

The coarse fraction resulted in higher extraction yields using ChCl/U20, while no substantial differences were observed for EtOH60 (see **Figure 2**). A likely explanation for the reduced extraction efficiency of the fine fraction with ChCl/U20 lies in its high viscosity. While smaller particles increase surface area, they also reduce the interstitial space between them, which hinders solvent penetration – especially for viscous solvents like DES[54]. Ethanol, being significantly less viscous, can diffuse more easily through these smaller gaps, which may explain the absence of significant differences in EtOH60 extractions across particle sizes. The differing performance was further evidenced by the longer vortexing time required for powder dispersion in ChCl/U20 samples, as the compacted powder-pellet was more difficult to disintegrate upon solvent addition. These observations suggest that particle size should not be too small, particularly if using ChCl/U20, to maintain efficient solvent accessibility, despite the general benefits of increased surface area. While excluding the fine fraction could have minimized the negative impact of reduced solvent penetration of ChCl/U20, it would have led to unnecessary material loss. Therefore, we selected a combined particle size of ≤ 355 µm as the standard method, balancing efficiency and sustainability.

TPC in Orange Powder Remained Stable Over Four Weeks

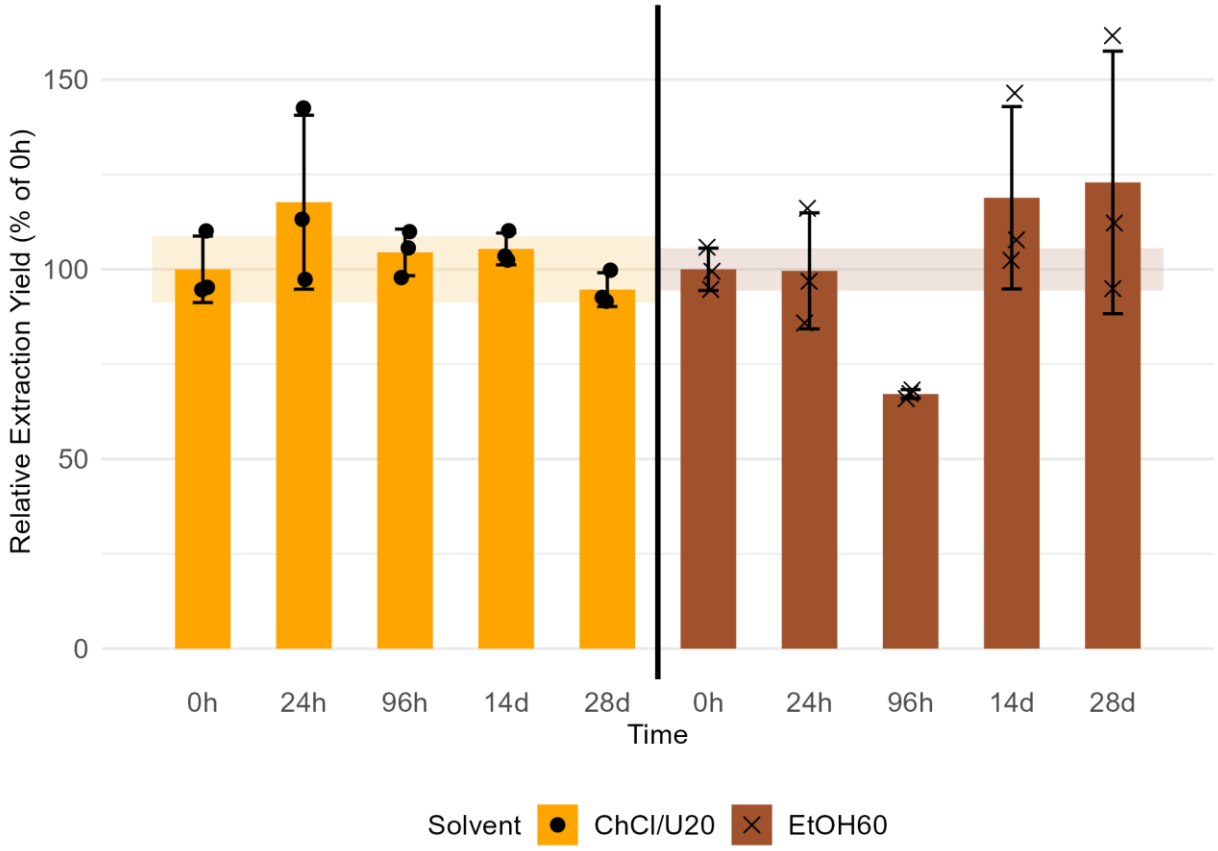

Figure 3: *Extraction yield (mg/gDW) from batch O.SAf (see* ***Table SI 2****) over a time period of 4 weeks using ChCl/U20 and EtOH60 with an S/L ratio of 1:5. Powder was stored in closed bottles under air, wrapped in aluminum foil. Bars represent the mean values ± standard deviation from three independent extractions. The shaded areas represent the technical SD at T0, used as a reference threshold for stability evaluation over time.*

To ensure comparability of the different orange powders used throughout the experiments, which were stored for up to three weeks, we assessed the stability of the phenolic content over a four-week period of one batch (see **Figure 3**). The majority of the measured values fall within the technical SD at T0, as represented by the shaded areas. The consistently low TPC values observed in the 96-hour EtOH60 samples are most likely due to a technical error during sample preparation or measurement. Since all three replicates were equally affected, a pipetting error – either during extraction (e.g., slightly overdrawing solvent relative to the powder) or during the 100-fold dilution prior to UV-Vis measurement – appears to be the most plausible

explanation. A degradation or compositional shift in phenolic compounds seems unlikely, as TPC values in EtOH60 samples returned to the expected range at later time points, and DES extracts did not show a similar drop at 96 hours. Variation in the EtOH60 samples at 14 and 28 days and ChCl/U20 24h was higher, each time influenced by a single outlier, which also raised the mean above the SD T0 range.

The experiment was conducted using a 1:5 S/L ratio prior to the identification of 1:10 as the optimal ratio, which could account for these observed outliers. Nevertheless, considering the technical SD, we can assume that the phenolic content remained stable throughout the investigation.

Natural Variation in TPC and Individual Flavonoids

Building on the initial optimization of total phenolic extraction and measurement, we examined whether different orange peel batches are equally suitable sources of flavonoids intended for pesticidal applications. We analyzed both intra- and inter-batch variability in TPC and, in contrast to the first part, additionally determined the specific composition and quantity of individual flavonoids. This allowed us not only to assess the consistency of different orange sources, but also to gain insight into how well TPC reflects actual flavonoid yield.

Slightly Greater Variation in Phenolic Yield Between Different Batches Than Within a Single Batch

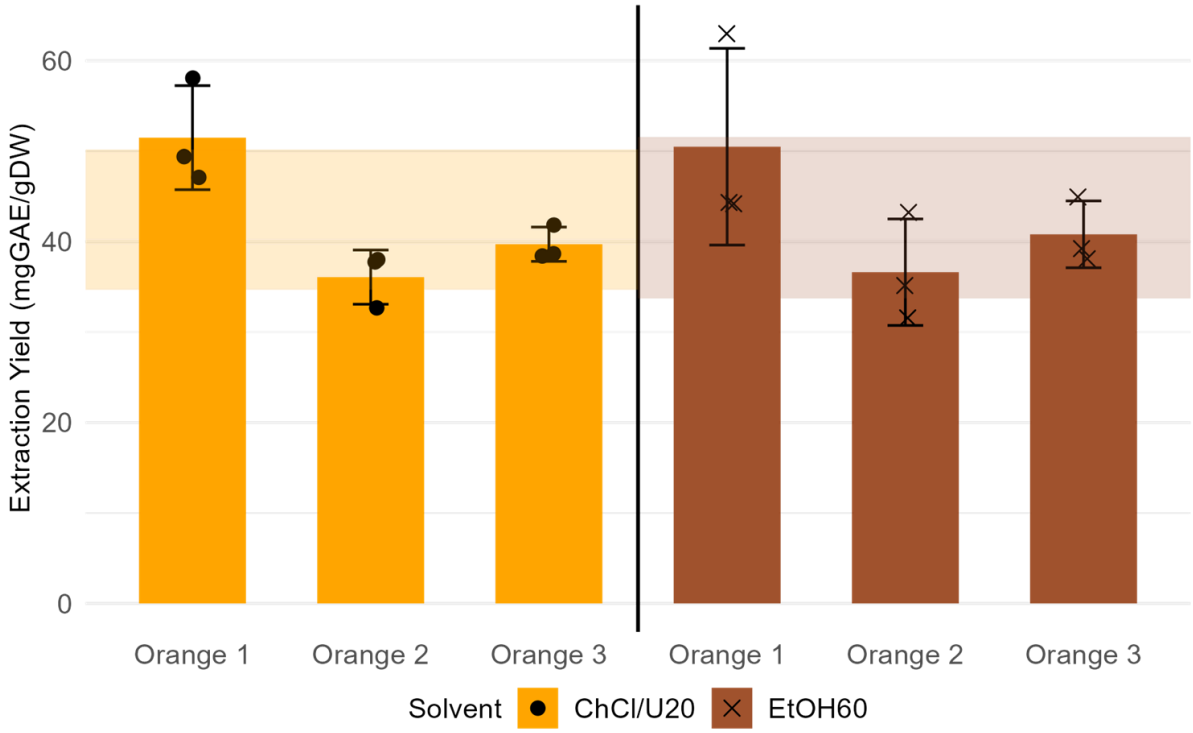

Figure 4: *TPC (mgGAE/gDW) extracted of three different oranges from the same batch (conventional orange, country Botswana (see* ***Table SI 2****)) using ChCl/U20 and EtOH60 with an S/L ratio of 1:10. Bars represent the mean values ± standard deviation from three independent extractions. The shaded areas indicate the mean ± relative standard deviation (RSD: ChCl/U20: 18.28%, EtOH60: 20.92%) across all samples for each solvent.*

The phenolic content of orange peels from the same batch were 42.64 ± 8.92 and 42.43 ± 7.76 mg GAE/g DW for EtOH60 and ChCl/U20, respectively (see **Figure 4**). Notably, nearly identical mean extraction yields were obtained for each of the three oranges, regardless of whether ChCl/U20 or EtOH60 was used. The RSD for technical replicates ranges from about 5% to 20%. Considering this, a large part of the measured biological variance (RSD: 20.92% for EtOH60 and 18.28% for ChCl/U20) between the three oranges can already be attributed to technical variability, indicating that the biological variance within the batch is low.

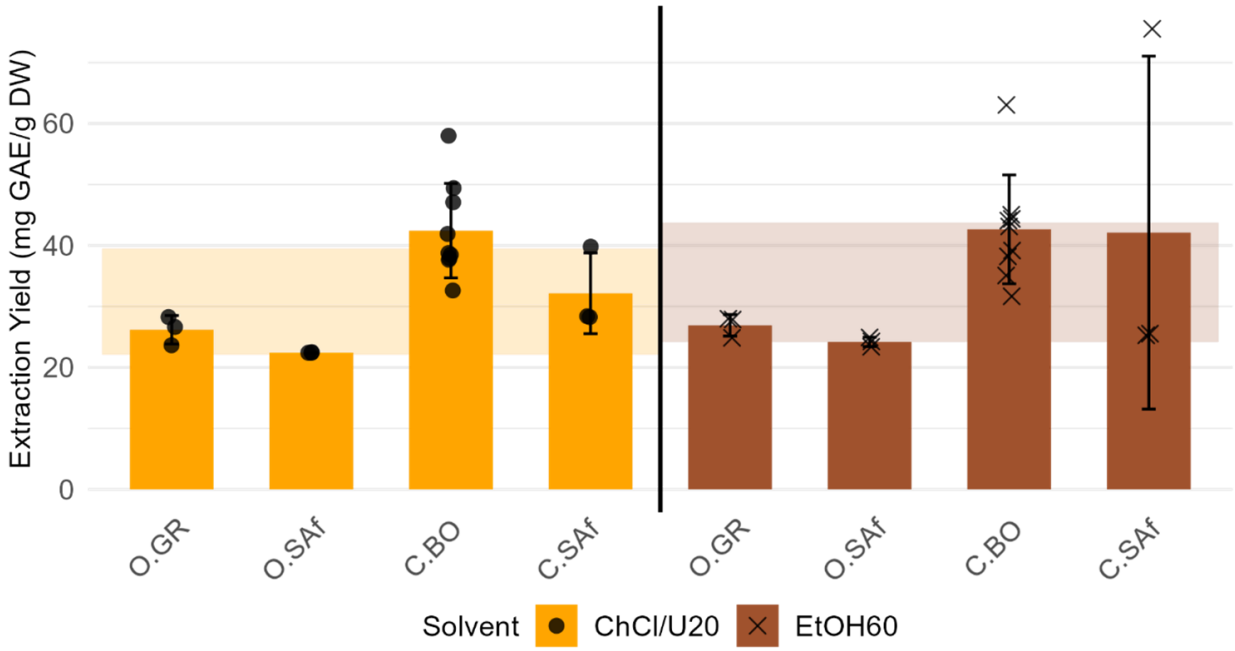

Figure 5: *Extraction yield (mg GAE/g DW) of phenolic compounds from orange samples originating from Botswana, Greece, and South Africa (see* ***Table SI 2****) using ChCl/U20 and EtOH60, with an S/L ratio of 1:10. Bars represent the mean values ± standard deviation from independent extractions. For most samples, mean values were calculated from triplicate measurements; for samples from Botswana, nine measurements were used to calculate the mean. The shaded areas indicate the mean ± relative standard deviation (RSD: ChCl/U20: 28.34%, EtOH60: 28.82%) across all samples for each solvent.*

Next, we examined the phenolic content variability between different orange batches. Therefore, three additional batches were included. Three mixed powders were produced from three oranges of each batch. These were then compared with the mean value of the intra-batch measurement (C.BO) (see **Figure 5**). The mean TPC was 30.80 ± 8.73 (RSD: 28.34%) and 33.96 ± 9.79 (RSD: 28.82%) mgGAE/gDW for ChCl/U20 and EtOH60, respectively. The results suggest that, although overall variability in TPC is relatively low, it appears to be slightly more influenced by differences between orange batches than by variation within a single batch. This is reflected not only in the higher RSD values across batches compared to the lower intra-batch RSDs (see **Figure 4**), but also in the range of mean TPC values, which spans from 22.43 to 42.64 mg/g DW. Nevertheless, the observed variance remains well below that reported in the literature.

The nearly identical RSD values for both solvents indicate that the choice of solvent has a minimal impact on extraction variability. Instead, the observed moderate differences are more likely attributable to batch-specific factors such as cultivation conditions, geographic origin, fertilization practices, or post-harvest storage, rather than the extraction method itself. This is also supported by the observation that conventional oranges tend to show higher TPC levels than organic ones. Additionally, an attempt was made to assess whether storage duration could explain the observed differences, based on estimated harvest seasons[55] and typical storage times (see **Table SI 2**): Batch O.GR was probably stored for several months after harvest, while O.SAf, C.SAf and C.BO were stored for a rather short time before being sold and processed into powder. However, batch O.SAf has similar TPC values to O.GR despite the short storage period. Batch C.SAf has a higher average TPC but is strongly influenced by an unexplained outlier for each solvent. Only batch C.BO, from the intra-batch evaluation, shows significantly higher TPC. This indicates that the storage differences play a minor role in the measured differences or that the estimates may be inaccurate. Another notable difference between organic and conventional samples is the variability in extraction yields. Organic samples consistently exhibited smaller error bars, whereas conventional samples showed higher variability.

Together, these findings highlight moderate differences between the orange batches in terms of phenolic content. Given the broad range of phenolic contents reported in the literature ranging from 0.6 – 30 mgGAE/gDW[37,42], the observed variations appear relatively minor. To further investigate whether conventional oranges are indeed more suitable for extractions intended for pesticidal applications, a closer examination of the specific flavonoid composition is of interest. This is addressed in the following section.

Only Hesperidin and Naringin Detected Among Targeted Glycosylated Flavanones

To investigate the exact composition of flavonoids in the analyzed orange peel samples, UHPLC-HRMS analysis was performed. The exact same extracts analyzed for TPC were used to enable direct comparison.

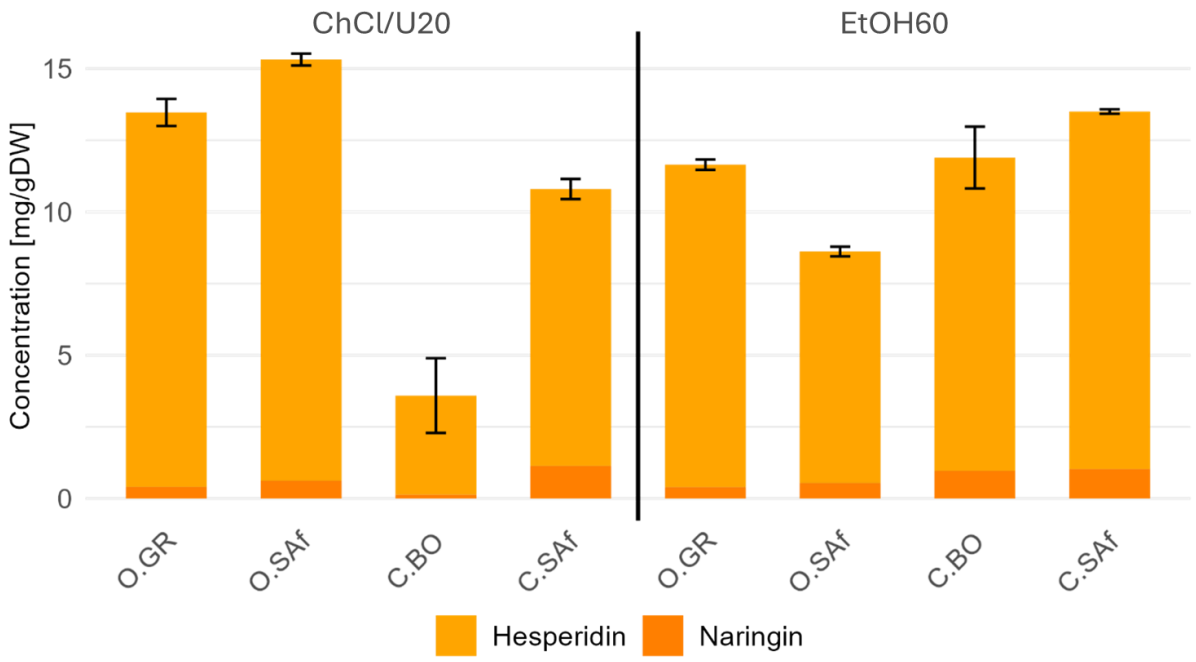

Figure 6: *Extraction yield (mg/g DW) of glycosylated flavonoids from orange samples originating from Botswana, Greece, and South Africa (see* ***Table SI 2****) using ChCl/U20 and EtOH60 as solvents, with an S/L ratio of 1:10. Bars represent mean values calculated from triplicate measurements for Greece and South Africa samples, and from nine replicates for Botswana samples from independent extractions. The mean glycosylated flavonoid concentration for each flavanone was calculated, and error bars indicate the standard deviation of the total glycosylated flavonoid concentration across the replicates. Hesperidin was quantified semi-quantitatively using the naringin calibration curve, applying a correction factor of 2.21 as described in the Methods section (see* ***Figure SI 3****). Chemical structures of the quantified flavanones are shown in* ***Table 1****.*

A targeted search for various glycosylated flavonoids was conducted using available analytical standards (see **Table SI 6**). As expected, hesperidin was the most abundantly extracted flavonoid across all citrus samples, confirming its dominance in citrus peels[56–58], with mean values of 10.22 ± 4.97 mg/g DW and 10.69 ± 1.86 mg/g DW for all oranges extracted with ChCl/U20 and EtOH60, respectively. Naringin was found at average concentrations of 0.57 ± 0.43 mg/g DW and 0.73 ± 0.31 mg/g DW for ChCl/U20 and EtOH60, respectively. Both flavonoids were confirmed through MS2 spectra (see **Figure SI 20** and **Figure SI 21**). Rutin was also monitored but detected only in trace amounts, insufficient for quantification. The RSD for the total glycosylated flavonoid means is 46.24% for ChCl/U20 and 16.52% for EtOH60.

The high RSD for ChCl/U20 is primarily driven by the low concentration of glycosylated flavonoids measured in the C.BO batch, which significantly influences the overall variability in the data.

Interestingly, while TPC appeared consistent between solvents within each orange batch, the quantification of glycosylated flavonoids revealed substantial solvent-dependent variation. These differences are not reflected in the overall means per solvent but become evident when comparing the individual batch means for each solvent (see **Figure 6)**. This contrast reveals solvent-specific extraction efficiencies hidden in the TPC data and underscores the importance of compound-level analysis. Consequently, no general conclusion can be drawn at this stage regarding the superior suitability of conventional orange peels for pesticidal use, as might have been assumed based on TPC measurements. Similarly to TPC yields, no consistent relationship with storage duration of the orange batches was observed.

In literature, DESs such as ChCl/U20 are often considered more efficient than ethanol for extracting polar compounds like glycosylated flavonoids due to their higher polarity and hydrogen-bonding capacity[41]. However, our results showed no clear solvent advantage. Rather than confirming a clear advantage of ChCl/U20, the yields of hesperidin and naringin varied depending on both the extraction solvent and the cultivation method of the oranges. ChCl/U20 resulted in moderately higher hesperidin yields in organically grown oranges, while EtOH60 was slightly more effective in conventionally grown oranges. A similar trend was observed for naringin, with the exception of the South African conventional sample (C.SAf), which showed higher yields with ChCl/U20 (see **Figure 6**).

Overall, glycosylated flavonoid yields across all samples ranged mostly between approximately 8–15 mg/g DW. This is generally in agreement with literature yields, where methanol and ethanol extractions typically result in hesperidin contents ranging from approximately 9–35 mg/g DW[40], 3–13 mg/g DW[37], and 1 mg/g FW (~4 mg/g DW) for hesperidin and 0.3 mg/g FW (~1.2 mg/g DW) for naringin as reported by Khan et al.[53] (assuming a 75% moisture loss during drying). Sawalha et al.[58] reported up to 35 mg/g DW hesperidin using methanol, while Xu et al.[41] obtained 25–35 mg/g DW hesperidin with various DES combinations.

Predominance of Fully Methoxylated Flavones

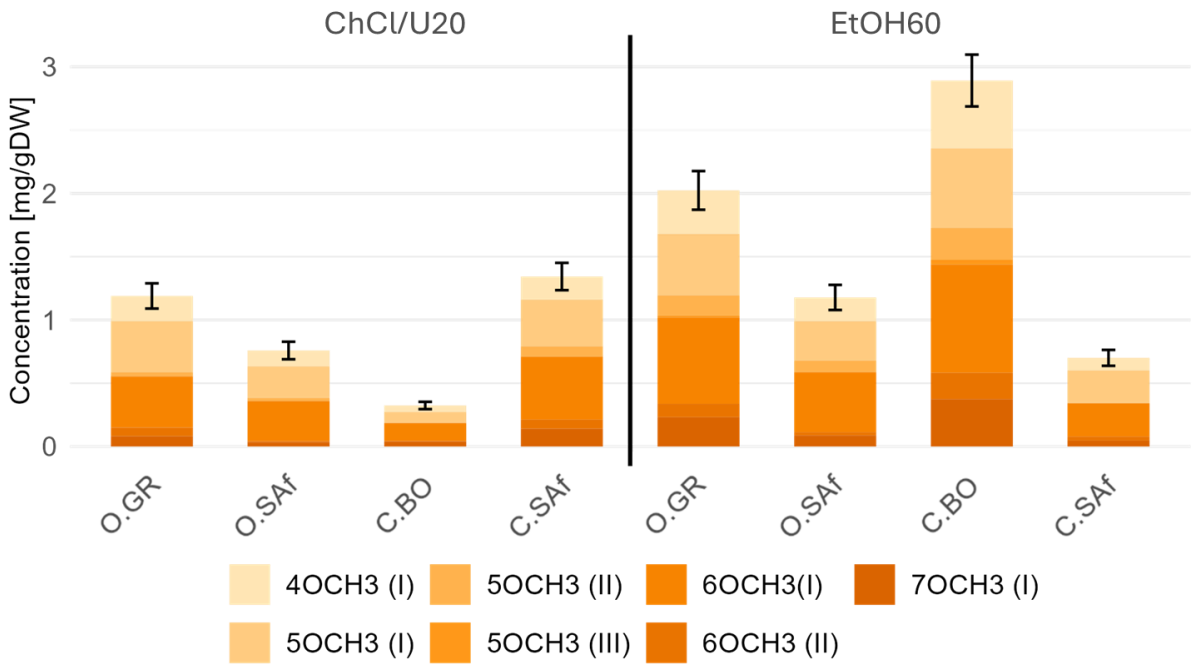

Figure 7: *Extraction yield (mg/g DW) of PMFs from orange samples originating from Botswana, Greece, and South Africa (see* ***Table SI 2****) using ChCl/U20 and EtOH60 as solvents, with an S/L ratio of 1:10. Bars represent mean values calculated from triplicate measurements for Greece and South Africa samples, and from nine replicates for Botswana samples from independent extractions. The mean PMF concentration for each flavonoid was calculated, and error bars indicate the standard deviation of the total PMF concentration across the replicates. Labels (I), (II), and (III) represent PMFs with the same number of OMe but different substitution patterns, as evidenced by their distinct retention times. Representative chemical structures of fully methoxylated flavones with 4–7 OMe are shown in* ***Table 1****.*

Additionally, we screened for PMFs with varying degrees of hydroxylation (see **Table SI 7**). The total PMF concentrations across the orange batches were 0.90 ± 0.46 mg/g DW (RSD: 50.79%) and 1.70 ± 0.97 mg/g DW (RSD: 56.86%) for ChCl/U20 and EtOH60, respectively. Under the applied extraction and analytical conditions (dilution of 1:250), we consistently detected PMFs with at least 4 OMe and without hydroxyl groups (see **Figure SI 13 - 19**). This aligns with the literature where PMFs substituted with ≥ 4 OMe are described as dominant in citrus peels[21]. PMFs with identical numbers of OMe but varying substitution patterns were detected based on distinct retention times. However, their exact structures was not determined.

The largest peaks correspond to compounds with five ($5OCH_3$ (I)) and six ($6OCH_3$ (I)) OMe and no hydroxyl substituents, and could be the PMFs tangeretin (5,6,7,8,4′-pentamethoxyflavone) and nobiletin (5,6,7,8,3′,4′-hexamethoxyflavone), respectively, which dominate in oranges according to the literature[21]. During method development, also hydroxylated flavonoids with one OH group were detectable at lower dilutions (1:20) in both ChCl/U20 and EtOH60 extracts (see **Figure SI 12**), suggesting that their actual concentrations are below the detection limit in the current setup.

EtOH60 exhibited a generally higher extraction efficiency for PMFs compared to ChCl/U20, except for the C.SAf samples. The highest total PMF concentration (~3 mg/g DW) was observed in the C.BO EtOH60 samples, where the extraction yielded nearly ten times more total PMFs than ChCl/U20 did. Similarly to the result for glycosylated flavonoids, this means that the quantification of individual flavonoids revealed substantial solvent-dependent variation while TPC-yields did not. Despite differences in absolute PMF yields, the relative proportions of individual PMFs remained almost similar across all samples, regardless of geographical origin or solvent (see **Figure SI 10**). This indicates that differences in extraction efficiency between EtOH60 and ChCl/U20 affect all PMFs to a similar extent, leading to comparable flavonoid profiles.

Relative Proportion of Flavonoids Within TPC

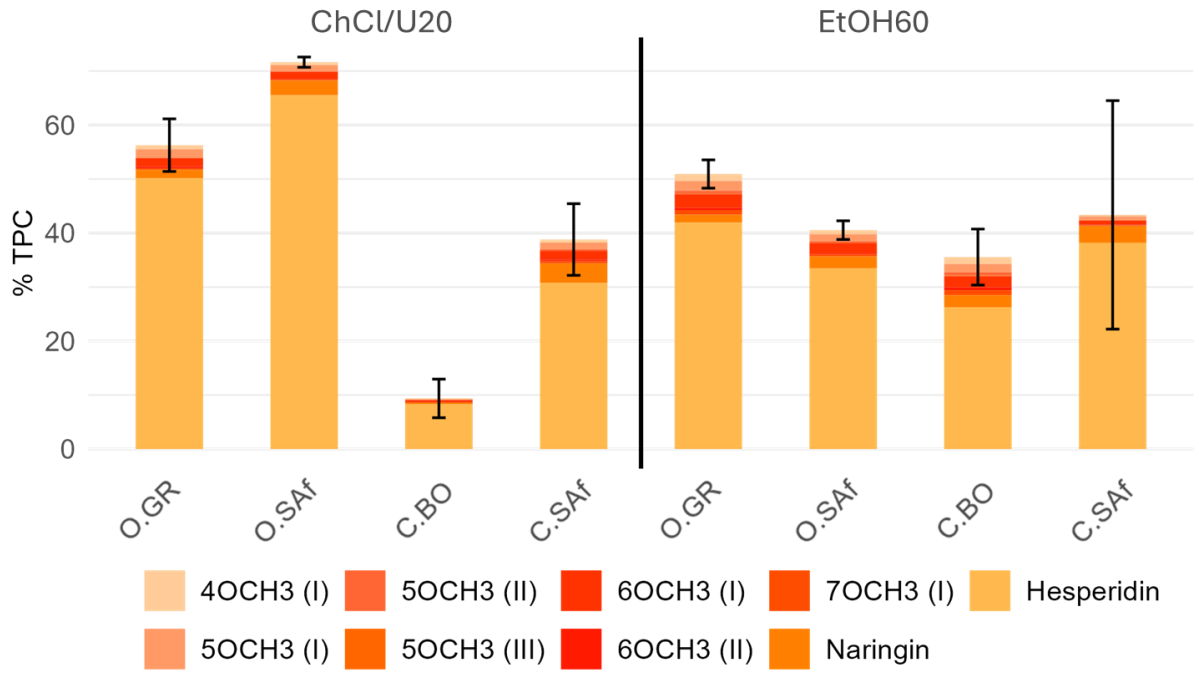

Figure 8: *Distribution of flavonoids, including PMFs and glycosylated flavonoids, expressed as a percentage of the TPC for orange samples from Botswana, Greece, and South Africa (see **Table SI 2**). The percentages were calculated based on previously determined TPC values for each sample, followed by determining the proportion of PMFs and glycosylated flavonoids. Mean percentages for each flavonoid were calculated from triplicate measurements for Greece and South Africa samples and nine replicates for Botswana samples for both solvents (ChCl/U20 and EtOH60). Error bars indicate the standard deviation of the total percentage of PMFs and glycosylated flavonoids relative to TPC across the replicates. Labels (I), (II), and (III) represent PMFs with the same number of OMe but different substitution patterns, as evidenced by their distinct retention times. Representative chemical structures of the identified flavonoids are shown in **Table 1.***

To determine the proportion of flavonoids relative to the TPC, the flavonoid yields were expressed as a percentage of the previously measured TPC. On average, the flavonoid content accounted for 44.03 ± 26.07% of the measured TPC in the ChCl/U20-extracted samples, while in the EtOH60-extracted samples, it represented 42.60 ± 6.42% of the TPC. As shown in **Figure 8**, the proportion of flavonoids in the TPC extracted with EtOH60 is relatively consistent across all samples (RSD: 15.07%). In contrast, the ChCl/U20 extractions display considerable variability (RSD: 59.21%), with flavonoids contributing between approximately

10% and 70% of the total TPC. This suggests that TPC may reflect general trends in flavonoid extraction but is ultimately too variable – especially with ChCl/U20 – to reliably indicate actual flavonoid content.

As mentioned in the introduction, approximately 70 million tons of oranges were produced globally in 2023[19], with an estimated 50-60% of the fruit mass typically discarded as peel – equivalent to 35-42 million tons. Assuming a dry matter content of 25%, this corresponds to up to 10 million tons of dry orange peel waste worldwide. Based on the extraction methods applied in this study using ChCl/U20 or EtOH60, average flavonoid yields of 11.70 and 13.12 g/kg DW were obtained, respectively (see **Table SI 8**). This corresponds to an estimated 123,800 tons of extractable flavonoids annually using ChCl/U20, though this estimate should be treated with caution given the greater variability associated with DES extractions. In contrast, EtOH60 yields are estimated to 138,800 tons and may be considered more consistent. While these figures represent a theoretical upper limit – assuming full global utilization – they nevertheless underscore the significant potential of citrus peel waste as a resource for natural pesticides.

Biotransformation of Flavonoids from Orange Peel Extract in Soil

A further focus of this study was the investigation of the persistence of our extracted flavonoids in soil. This represents a critical aspect, considering their potential use as biopesticides. A novel aspect of this study, is the application of the full orange peel extract into the soil. This mixture includes not only the investigated glycosylated flavonoids and PMFs, but also a variety of co-extracted, unidentified compounds such as other phenolics, potentially influencing the observed degradation processes. We conducted biodegradation experiments over three weeks in both microbially active (non-sterile) and autoclaved (sterile) soils to assess their transformation rates and determine whether this process is microbially driven.

Slower Transformation of Naringin and Hesperidin Compared to Pure Standards

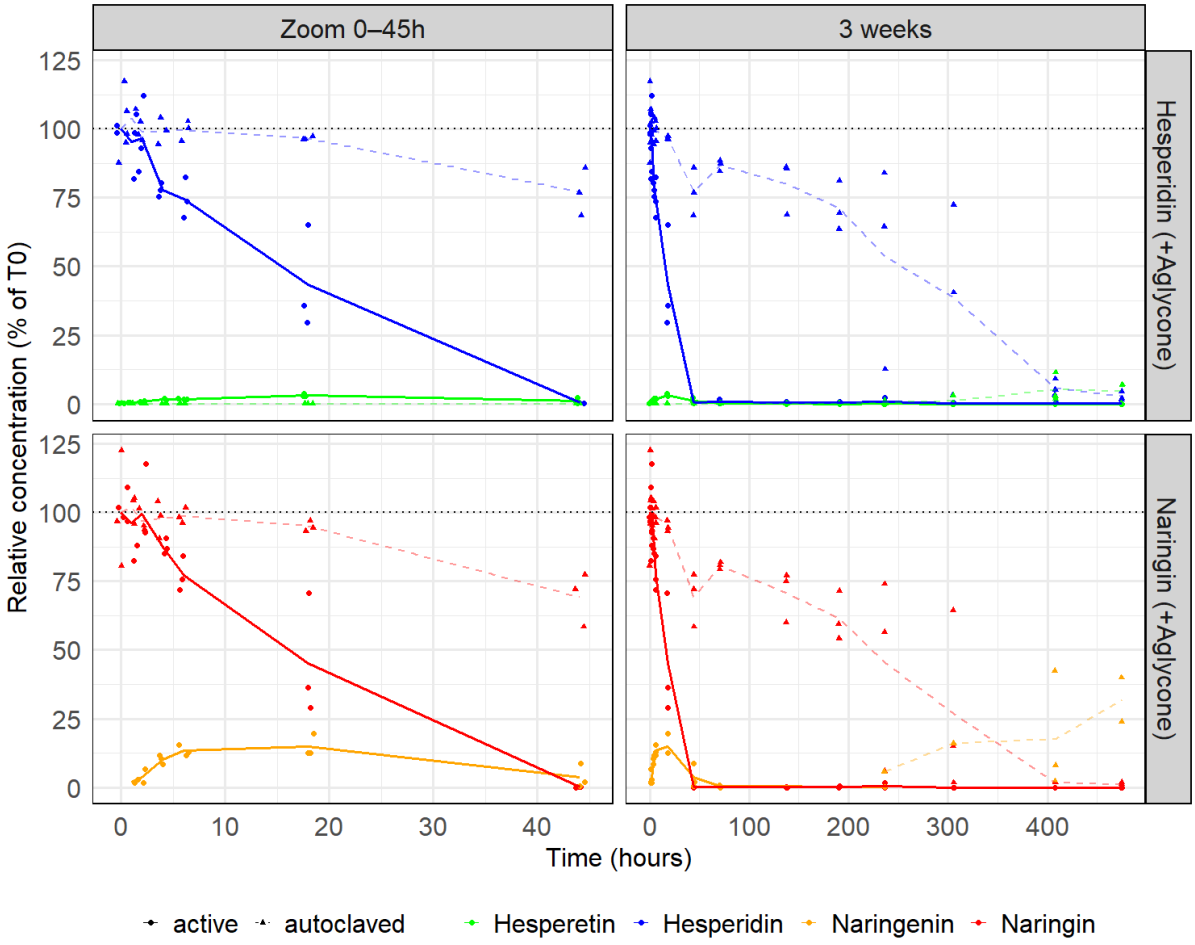

Figure 9: *Flavanone transformation in soil over a three-week period. The initial concentration (100%) refers to the mean of triplicate measurements at T0. At each time point, independent triplicate samples were analyzed. Lines represent the mean values at each time point and illustrate the transformation kinetics. The orange samples originated from organic cultivation in Italy (see* ***Table SI 2****). The flavonoid content of the stock solution, expressed in mg/gDW, is provided in the SI: glycosylated flavonoids and PMFs O.IT. Missing data points (e.g., for naringenin) indicate concentrations below the limit of detection (LOD). Chemical structures of the flavanones are shown in* ***Table 1****.*

Figure 9 illustrates the transformation profiles of hesperidin and naringin, alongside their respective aglycones, hesperetin and naringenin. Both glycosylated flavanones undergo rapid transformation in active soil (solid line) and were no longer detectable within two days (Zoom

0-45h). Under sterile conditions approximately 25% of the original compounds transformed (dashed line) within the same time frame. This indicates their low persistence and highlights that microbial activity is the key driver of their fast transformation.

As also observed by Gruseck et al., deglycosylation towards the aglycones is evident. After about 17 hours, peak concentrations of the aglycones were detected, with naringenin accounting for approximately 13 % and hesperetin for about 5 % of the initial glycoside levels. These values represent only transient concentrations, as the aglycones themselves continue to transform over time. In autoclaved soils, transformations occurred but at a slower rate, likely because sterilization did not fully eliminate microorganisms, allowing for gradual regrowth and delayed onset of transformation processes. Here, the aglycones became detectable only after about 10 days, by which time approximately 50 % of the glycosylated flavanones had already transformed. After three weeks, they reached ~30 % of the initial naringin and ~6 % of the initial hesperidin. This is a common pattern in the transformation of both compounds: hesperidin and naringin undergo enzymatic hydrolysis, most likely mediated by naringinase, an enzyme complex with α-L-rhamnosidase and β-glucosidase activity. This enzymatic process breaks down the rhamnose and glucose groups, leading to the transient formation of the aglycones hesperetin and naringenin[59]. However, these intermediates are short-lived, as they are rapidly metabolized further by microbial communities[12]. Their low detectability suggests immediate conversion into smaller metabolites, whose identities remain unknown.

Gruseck et al.[46] investigated, among other glycosylated flavonoids, the transformation of synthetic naringin, which showed 60% conversion within just 4 hours in the same soil when applied as a pure flavonoid solution. As shown in **Figure 9**, this was significantly faster than the microbial transformation of naringin when applied as part of the orange peel extract, where only ~15% transformation was observed after 4 hours. These findings suggest that additional co-extracted compounds may slow down the microbial transformation process.

Almost None to Slower Transformation of PMFs Compared to Pure Standards

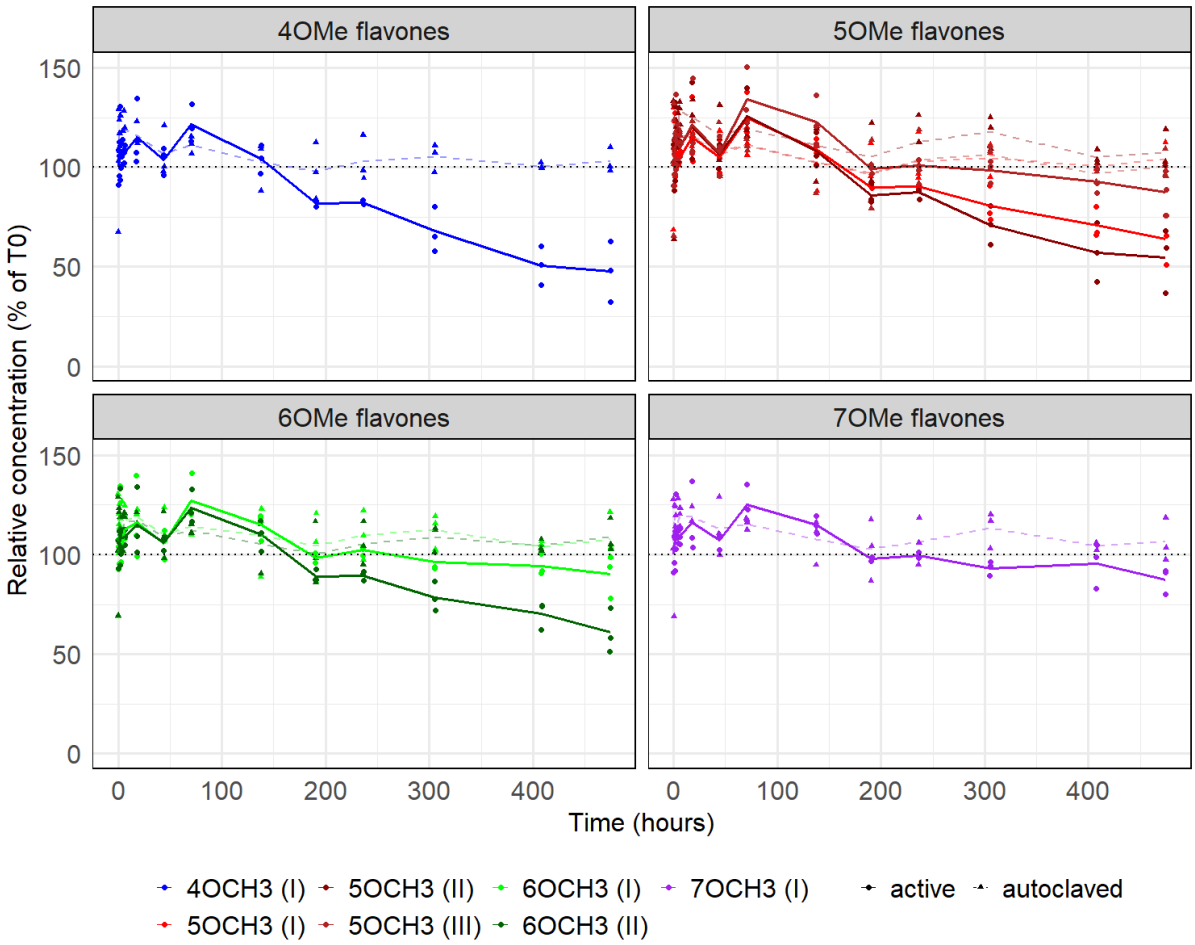

Figure 10: *PMF transformation in soil over a three-week period. The initial concentration (100%) refers to the mean of triplicate measurements at T0. At each time point, independent triplicate samples were analyzed. Lines represent the mean values at each time point and illustrate the transformation kinetics. The orange samples originated from organic cultivation in Italy (see* ***Table SI 2****). The flavonoid content of the stock solution, expressed in mg/gDW, is provided in the SI: glycosylated flavonoids and PMFs O.IT. Unlike the glycosylated flavonoids, no missing data points were observed in this dataset. Labels (I), (II), and (III) represent PMFs with the same number of OMe but different substitution patterns, as evidenced by their distinct retention times. Representative chemical structures of fully methoxylated flavones with 4–7 OMe are shown in* ***Table 1****.*

Over the course of 3 weeks, PMF transformation remains relatively low to moderate (~10–50 %) and clearly lower than that of glycosylated flavonoids. In active soil all compounds

exhibit an initial lag phase with slight fluctuations, while transformation typically begins after 6-8 days. In the autoclaved soil, all flavones remain stable.

Although PMFs may have the same number of OMe, transformation rates vary, indicating that the position of these substituents – rather than their number – is the main factor influencing microbial breakdown. This is evidenced by the different transformation curves of PMFs that are differentially substituted with five or six OMe each (see **Figure 10**). Some methoxy positions likely result in increased stability. The higher the number of OMe substituents the higher the chance of occupying such stabilizing sites. Gruseck et al. reported a half-life of 5.5 days in 5M soil for a PMF with four OMe[46], which was substituted differently than the compound in this study, as indicated by different retention times. In contrast, the PMF with four OMe examined here transformed to 50% only after 16.5 days. Additionally, unlike Gruseck et al., who observed a marked decrease in the concentration of all investigated PMFs, we found several PMFs that showed minimal or nearly no transformation over the 3-week study period. This suggests that transformation processes are likely slowed down by co-extracted compounds in the crude extracts. As a result, minimal or even negligible transformation of certain PMFs is observed – unlike the behavior for pure flavonoids. Additionally, differing substitution patterns complicate direct comparison with Gruseck et al., as the specific positioning of OMe appears to significantly influence microbial transformation. This highlights the importance of studying transformation in realistic, application-oriented mixtures.

To investigate potential demethylation as a transformation pathway – such as the conversion of 5-OCH_3 substituents into hydroxylated ones (e.g., 4OCH_3 + OH) – a suspect screening for potential demethylation products was conducted. However, no signals corresponding to such demethylation products were detected. While this suggests it is not a major pathway under the tested conditions, short-lived or low-abundance products cannot be ruled out.

The slight increase or fluctuation in PMF concentrations during the first few days could be explained by sorption-desorption dynamics rather than microbial activity, as a similar pattern was observed in autoclaved soils. At T0, a fraction of the PMFs may have adsorbed onto soil particles, leading to an initially underestimated concentration in solution. As desorption

occurred over the following days, this resulted in an apparent increase before stabilization or transformation began.

Taken together, the findings from our degradation experiment indicate that microbial transformation is the key driver in the degradation of both glycosylated flavonoids and PMFs. Compared to pure flavonoids[46], transformation rates in our extracts were slower, suggesting that co-extracted compounds may slow down microbial breakdown. This matrix effect could increase environmental residence time and thereby prolong potential pesticidal activity. Moreover, the results suggest that not the number but the position of OMe influences PMF stability, potentially offering structural control points to tune transformation kinetics and persistence in future formulations.

Conclusion

The extraction of flavonoids and phenols from peels from four tested orange batches revealed that their variability between batches was moderate – with RSDs of 28% for TPC and up to 50% for individual flavonoids – compared to the much higher variation observed across values reported in previous studies[36–42]. This suggests that natural variation plays a smaller role than could be assumed based on the fluctuations reported in literature. Therefore, discrepancies in published data might primarily be due to differences in extraction efficiency. No clear trend was observed indicating that certain orange batches are inherently more suitable for the extraction of flavonoids intended for biopesticide production. Instead, the results suggest that moderate differences already exist at the intra-batch level, as variability in TPC within the same batch was only slightly lower than that observed between different batches. Since this intra-batch variability is solely based on TPC measurements – which, as discussed below, may not reliably reflect flavonoid-specific differences – HPLC-HRMS-based quantification of individual flavonoids would be needed to substantiate this assumption.

The limitations of using TPC as a proxy for flavonoid content become evident when comparing inter-batch results from TPC and HPLC-HRMS analyses. Despite similar TPC yields between ChCl/U20 and EtOH60, HPLC-HRMS revealed more pronounced differences in flavonoid yields between the two solvents. The limitation is further supported by the flavonoid-to-TPC ratio: although, on average, about 40% of the measured TPC could be attributed to flavonoids, this ratio fluctuated substantially – particularly in ChCl/U20 samples. This highlights that similar TPC values do not necessarily reflect similar flavonoid yields, and that TPC measurements may, therefore, be misleading when used as a proxy for flavonoid content.

While Gruseck et al.[46] examined the transformation of pure flavonoids in soil, this work conducted soil incubation experiments investigating the transformation of flavonoids extracted from orange peel in the presence of co-extracted compounds. Our findings indicate that these background compounds can significantly slow down the transformation of individual flavonoids. Glycosylated flavonoids were completely microbially transformed within two days during soil incubation. In contrast, PMFs showed transformation extents ranging from almost 0% to 50% after three weeks. In addition to matrix effects, structural features of the flavonoids

themselves appeared to play a role: the position of OMe appeared to have a stronger influence on stability and transformation rate of PMFs than the number of OMe. Nonetheless, a higher number of OMe may increase the likelihood that key stabilizing positions are occupied. While Gruseck et al. observed at least partial transformation of all PMFs[46], some PMFs in this study showed almost no change in concentration during soil incubation. In their study, they also raised concerns about the rapid transformation of flavonoids during pesticide application. Our findings suggest that co-extracted compounds can decelerate these rapid transformation processes, potentially prolonging pesticidal effectiveness.

Apart from these findings, several limitations should be noted. Flavonoid stability in the powder over four weeks was monitored solely via TPC measurements, based on the assumption of a strong correlation with flavonoid content. However, since the stability of individual flavonoids was not assessed, their concentrations may have changed over time, even if TPC values remained constant. Likewise, intra-batch variation was only examined using TPC measurements. Given that this study showed TPC is not a reliable proxy for flavonoid content, repeating both the stability experiment and the intra-batch comparison using HPLC-HRMS analysis of individual flavonoids is essential to obtain more accurate insights.

To further understand the biotransformation of PMFs in combination with co-extracted compounds, future studies should extend the monitoring period to at least three months. Given that only up to 50% transformation was observed within the first three weeks, longer-term data are needed to determine whether and when complete transformation occurs. Additionally, controlled incubation experiments using synthetic PMFs with varying numbers and known positions of OMe could help clarify the relationship between chemical structure and microbial transformation. Similar insights could also be gained through detailed identification of PMFs in the extract, particularly regarding the specific location of OMe groups. MS/MS-based analysis using diagnostic product ions[51] could help determine whether OMe are located on the A- or B-ring of the flavonoid core structure.

To isolate the effects of co-extracted compounds on transformation behavior, glycosylated flavonoids and PMFs could be separated from the extract using preparative high-speed counter-current chromatography followed by preparative HPLC[60]. Testing these compounds both in their isolated form and within the full extract mixture would allow for a more precise

assessment of matrix effects on biotransformation dynamics. In addition, a non-targeted analysis of the orange peel extract may help identify further compounds that influence the microbial transformation of flavonoids. Beyond these follow-up approaches, potential effects of the extracts on target pathogens are highly relevant in the context of pesticidal application.

As already detailed in this study, globally over 100,000 tons of flavonoids can be extracted from orange peel waste. The comparison of yields from batches examined in this study supports the idea that commercial orange varieties tend to exhibit flavonoid yields with only moderate variation. Along with improved knowledge of their transformation kinetics influenced by co-extracted compounds, these findings underscore the suitability of orange peel waste as a source of sustainable pesticide alternatives, with the potential to be part of a gradual replacement of synthetic chemical pesticides.

Bibliography

(1) Food and Agriculture Organization of the United Nations (FAO). Pesticides Use and Trade 1990–2021, 2022. https://openknowledge.fao.org/server/api/core/bitstreams/222f250c-3764-401b-98c7-f52a699dd65c/content.

(2) Delcour, I.; Spanoghe, P.; Uyttendaele, M. Literature Review: Impact of Climate Change on Pesticide Use. *Food Research International* **2015**, *68*, 7–15. https://doi.org/10.1016/j.foodres.2014.09.030.

(3) Silva, V.; Mol, H. G. J.; Zomer, P.; Tienstra, M.; Ritsema, C. J.; Geissen, V. Pesticide Residues in European Agricultural Soils – A Hidden Reality Unfolded. *Science of The Total Environment* **2019**, *653*, 1532–1545. https://doi.org/10.1016/j.scitotenv.2018.10.441.

(4) Riedo, J.; Wettstein, F. E.; Rösch, A.; Herzog, C.; Banerjee, S.; Büchi, L.; Charles, R.; Wächter, D.; Martin-Laurent, F.; Bucheli, T. D.; Walder, F.; Van Der Heijden, M. G. A. Widespread Occurrence of Pesticides in Organically Managed Agricultural Soils—the Ghost of a Conventional Agricultural Past? *Environ. Sci. Technol.* **2021**, *55* (5), 2919–2928. https://doi.org/10.1021/acs.est.0c06405.

(5) AbuQamar, S. F.; El-Saadony, M. T.; Alkafaas, S. S.; Elsalahaty, M. I.; Elkafas, S. S.; Mathew, B. T.; Aljasmi, A. N.; Alhammadi, H. S.; Salem, H. M.; Abd El-Mageed, T. A.; Zaghloul, R. A.; Mosa, W. F. A.; Ahmed, A. E.; Elrys, A. S.; Saad, A. M.; Alsaeed, F. A.; El-Tarabily, K. A. Ecological Impacts and Management Strategies of Pesticide Pollution on Aquatic Life and Human Beings. *Marine Pollution Bulletin* **2024**, *206*, 116613. https://doi.org/10.1016/j.marpolbul.2024.116613.

(6) Ganaie, M. I.; Jan, I.; Mayer, A. N.; Dar, A. A.; Mayer, I. A.; Ahmed, P.; Sofi, J. A. Health Risk Assessment of Pesticide Residues in Drinking Water of Upper Jhelum Region in Kashmir Valley-India by GC-MS/MS. *International Journal of Analytical Chemistry* **2023**, *2023*, 1–16. https://doi.org/10.1155/2023/6802782.

(7) Kiefer, K.; Müller, A.; Singer, H.; Hollender, J. New Relevant Pesticide Transformation Products in Groundwater Detected Using Target and Suspect Screening for Agricultural and Urban Micropollutants with LC-HRMS. *Water Research* **2019**, *165*, 114972. https://doi.org/10.1016/j.watres.2019.114972.

(8) Imfeld, G.; Vuilleumier, S. Measuring the Effects of Pesticides on Bacterial Communities in Soil: A Critical Review. *European Journal of Soil Biology* **2012**, *49*, 22–30. https://doi.org/10.1016/j.ejsobi.2011.11.010.

(9) Sim, J. X. F.; Doolette, C. L.; Vasileiadis, S.; Drigo, B.; Wyrsch, E. R.; Djordjevic, S. P.; Donner, E.; Karpouzas, D. G.; Lombi, E. Pesticide Effects on Nitrogen Cycle Related Microbial Functions and Community Composition. *Science of The Total Environment* **2022**, *807*, 150734. https://doi.org/10.1016/j.scitotenv.2021.150734.

(10) Lavin, K. S.; Hageman, K. J. Contributions of Long-Range and Regional Atmospheric Transport on Pesticide Concentrations along a Transect Crossing a Mountain Divide. *Environmental Science & Technology* **2013**, *47*, 1390–1398. https://doi.org/10.1021/es304497e.

(11) Daraban, G. M.; Hlihor, R.-M.; Suteu, D. Pesticides vs. Biopesticides: From Pest Management to Toxicity and Impacts on the Environment and Human Health. *Toxics* **2023**, *11* (12), 983. https://doi.org/10.3390/toxics11120983.
(12) Schnarr, L.; Olsson, O.; Kümmerer, K. Biodegradation of Flavonoids – Influences of Structural Features. *Chemosphere* **2024**, *359*, 142234. https://doi.org/10.1016/j.chemosphere.2024.142234.
(13) Schnarr, L.; Segatto, M. L.; Olsson, O.; Zuin, V. G.; Kümmerer, K. Flavonoids as Biopesticides – Systematic Assessment of Sources, Structures, Activities and Environmental Fate. *Science of The Total Environment* **2022**, *824*, 153781. https://doi.org/10.1016/j.scitotenv.2022.153781.
(14) Ramaroson, M.-L.; Koutouan, C.; Helesbeux, J.-J.; Le Clerc, V.; Hamama, L.; Geoffriau, E.; Briard, M. Role of Phenylpropanoids and Flavonoids in Plant Resistance to Pests and Diseases. *Molecules* **2022**, *27* (23), 8371. https://doi.org/10.3390/molecules27238371.
(15) Yang, F.; Shen, H.; Huang, T.; Yao, Q.; Hu, J.; Tang, J.; Zhang, R.; Tong, H.; Wu, Q.; Zhang, Y.; Su, Q. Flavonoid Production in Tomato Mediates Both Direct and Indirect Plant Defences against Whiteflies in Tritrophic Interactions. *Pest Management Science* **2023**, *79* (11), 4644–4654. https://doi.org/10.1002/ps.7667.
(16) Altunayar-Unsalan, C.; Unsalan, O.; Mavromoustakos, T. Insights into Molecular Mechanism of Action of Citrus Flavonoids Hesperidin and Naringin on Lipid Bilayers Using Spectroscopic, Calorimetric, Microscopic and Theoretical Studies. *Journal of Molecular Liquids* **2022**, *347*, 118411. https://doi.org/10.1016/j.molliq.2021.118411.
(17) Guo, L.; Mao, X.; Li, Y.; Zhou, Z. Polymethoxylated Flavonoids (PMFs)-Loaded Citral Nanoemulsion Controls Green Mold in Citrus by Damaging the Cell Membrane of Penicillium Digitatum. *Fungal Biology* **2023**, *127* (1–2), 854–864. https://doi.org/10.1016/j.funbio.2022.12.003.
(18) Salas, M. P.; Pok, P. S.; Resnik, S. L.; Pacin, A.; Munitz, M. Use of Citrus Flavanones to Prevent Aflatoxin Contamination Using Response Surface Methodology. *Food Control* **2016**, *60*, 533–537. https://doi.org/10.1016/j.foodcont.2015.08.026.
(19) Food and Agriculture Organization of the United Nations. FAOSTAT: Crops and Livestock Products, 2025. https://www.fao.org/faostat/en/#data/QCL.
(20) Satari, B.; Karimi, K. Citrus Processing Wastes: Environmental Impacts, Recent Advances, and Future Perspectives in Total Valorization. *Resources, Conservation and Recycling* **2018**, *129*, 153–167. https://doi.org/10.1016/j.resconrec.2017.10.032.
(21) Li, S.; Pan, M.-H.; Wang, Z.; Lambros, T.; Ho, C.-T. Biological Activity, Metabolism and Separation of Polymethoxyflavonoids from Citrus Peels. *Tree and Forestry Science and Biotechnology* **2008**, No. 1.
(22) Manthey, J. A.; Grohmann, K. Phenols in Citrus Peel Byproducts. Concentrations of Hydroxycinnamates and Polymethoxylated Flavones in Citrus Peel Molasses. *J. Agric. Food Chem.* **2001**, *49* (7), 3268–3273. https://doi.org/10.1021/jf010011r.
(23) Bergwerf, H. *MolView*. MolView. https://molview.org/.
(24) Wawoczny, A.; Gillner, D. The Most Potent Natural Pharmaceuticals, Cosmetics, and Food Ingredients Isolated from Plants with Deep Eutectic Solvents. *J. Agric. Food Chem.* **2023**, *71* (29), 10877–10900. https://doi.org/10.1021/acs.jafc.3c01656.

(25) Abbott, A. P.; Capper, G.; Davies, D. L.; Rasheed, R. K.; Tambyrajah, V. Novel Solvent Properties of Choline Chloride/Urea Mixtures. *Chem. Commun.* **2003**, No. 1, 70–71. https://doi.org/10.1039/b210714g.
(26) Mansur, A. R.; Song, N.-E.; Jang, H. W.; Lim, T.-G.; Yoo, M.; Nam, T. G. Optimizing the Ultrasound-Assisted Deep Eutectic Solvent Extraction of Flavonoids in Common Buckwheat Sprouts. *Food Chemistry* **2019**, *293*, 438–445. https://doi.org/10.1016/j.foodchem.2019.05.003.
(27) Nam, M. W.; Zhao, J.; Lee, M. S.; Jeong, J. H.; Lee, J. Enhanced Extraction of Bioactive Natural Products Using Tailor-Made Deep Eutectic Solvents: Application to Flavonoid Extraction from Flos Sophorae. *Green Chem.* **2015**, *17* (3), 1718–1727. https://doi.org/10.1039/C4GC01556H.
(28) Paradiso, V. M.; Clemente, A.; Summo, C.; Pasqualone, A.; Caponio, F. Towards Green Analysis of Virgin Olive Oil Phenolic Compounds: Extraction by a Natural Deep Eutectic Solvent and Direct Spectrophotometric Detection. *Food Chemistry* **2016**, *212*, 43–47. https://doi.org/10.1016/j.foodchem.2016.05.082.
(29) Hammond, O. S.; Bowron, D. T.; Edler, K. J. Liquid Structure of the Choline Chloride-Urea Deep Eutectic Solvent (Reline) from Neutron Diffraction and Atomistic Modelling. *Green Chem.* **2016**, *18* (9), 2736–2744. https://doi.org/10.1039/C5GC02914G.
(30) Nejrotti, S.; Antenucci, A.; Pontremoli, C.; Gontrani, L.; Barbero, N.; Carbone, M.; Bonomo, M. Critical Assessment of the Sustainability of Deep Eutectic Solvents: A Case Study on Six Choline Chloride-Based Mixtures. *ACS Omega* **2022**, *7* (51), 47449–47461. https://doi.org/10.1021/acsomega.2c06140.
(31) Lapeña, D.; Errazquin, D.; Lomba, L.; Lafuente, C.; Giner, B. Ecotoxicity and Biodegradability of Pure and Aqueous Mixtures of Deep Eutectic Solvents: Glyceline, Ethaline, and Reline. *Environ Sci Pollut Res* **2021**, *28* (7), 8812–8821. https://doi.org/10.1007/s11356-020-11144-w.
(32) Wen, Q.; Chen, J.-X.; Tang, Y.-L.; Wang, J.; Yang, Z. Assessing the Toxicity and Biodegradability of Deep Eutectic Solvents. *Chemosphere* **2015**, *132*, 63–69. https://doi.org/10.1016/j.chemosphere.2015.02.061.
(33) Smith, E. L.; Abbott, A. P.; Ryder, K. S. Deep Eutectic Solvents (DESs) and Their Applications. *Chem. Rev.* **2014**, *114* (21), 11060–11082. https://doi.org/10.1021/cr300162p.
(34) Zhao, B.-Y.; Xu, P.; Yang, F.-X.; Wu, H.; Zong, M.-H.; Lou, W.-Y. Biocompatible Deep Eutectic Solvents Based on Choline Chloride: Characterization and Application to the Extraction of Rutin from *Sophora Japonica*. *ACS Sustainable Chem. Eng.* **2015**, *3* (11), 2746–2755. https://doi.org/10.1021/acssuschemeng.5b00619.
(35) Haya, S.; Bentahar, F.; Trari, M. Optimization of Polyphenols Extraction from Orange Peel. *Food Measure* **2019**, *13* (1), 614–621. https://doi.org/10.1007/s11694-018-9974-2.
(36) Ozturk, B.; Parkinson, C.; Gonzalez-Miquel, M. Extraction of Polyphenolic Antioxidants from Orange Peel Waste Using Deep Eutectic Solvents. *Separation and Purification Technology* **2018**, *206*, 1–13. https://doi.org/10.1016/j.seppur.2018.05.052.
(37) Athanasiadis, V.; Chatzimitakos, T.; Kotsou, K.; Palaiogiannis, D.; Bozinou, E.; Lalas, S. I. Optimization of the Extraction Parameters for the Isolation of Bioactive Compounds from Orange Peel Waste. *Sustainability* **2022**, *14* (21), 13926. https://doi.org/10.3390/su142113926.

(38) Shamloo, M. M.; Sharifani, M.; Daraei Garmakhany, A.; Seifi, E. Alternation of Secondary Metabolites and Quality Attributes in Valencia Orange Fruit (Citrus Sinensis) as Influenced by Storage Period and Edible Covers. *J Food Sci Technol* **2015**, *52* (4), 1936–1947. https://doi.org/10.1007/s13197-013-1207-4.
(39) Bajkacz, S.; Adamek, J. Development of a Method Based on Natural Deep Eutectic Solvents for Extraction of Flavonoids from Food Samples. *Food Anal. Methods* **2018**, *11* (5), 1330–1344. https://doi.org/10.1007/s12161-017-1118-5.
(40) Victor, M. M.; David, J. M.; Cortez, M. V. M.; Leite, J. L.; Da Silva, G. S. B. A High-Yield Process for Extraction of Hesperidin from Orange (Citrus Sinensis L. Osbeck) Peels Waste, and Its Transformation to Diosmetin, A Valuable and Bioactive Flavonoid. *Waste Biomass Valor* **2021**, *12* (1), 313–320. https://doi.org/10.1007/s12649-020-00982-x.
(41) Xu, M.; Ran, L.; Chen, N.; Fan, X.; Ren, D.; Yi, L. Polarity-Dependent Extraction of Flavonoids from Citrus Peel Waste Using a Tailor-Made Deep Eutectic Solvent. *Food Chemistry* **2019**, *297*, 124970. https://doi.org/10.1016/j.foodchem.2019.124970.
(42) Li, B. B.; Smith, B.; Hossain, Md. M. Extraction of Phenolics from Citrus Peels. *Separation and Purification Technology* **2006**, *48* (2), 182–188. https://doi.org/10.1016/j.seppur.2005.07.005.
(43) Carlsen, S. C. K.; Pedersen, H. A.; Spliid, N. H.; Fomsgaard, I. S. Fate in Soil of Flavonoids Released from White Clover (*Trifolium Repens* L.). *Applied and Environmental Soil Science* **2012**, *2012*, 1–10. https://doi.org/10.1155/2012/743413.
(44) Furbo, S.; Mortensen, A. G.; Laursen, B.; Christophersen, C.; Fomsgaard, I. S. Degradation of Biochanin A in Soil. *Chemoecology* **2011**, *21* (2), 59–66. https://doi.org/10.1007/s00049-010-0066-y.
(45) Shaw, L. J.; Hooker, J. E. The Fate and Toxicity of the Flavonoids Naringenin and Formononetin in Soil. *Soil Biology and Biochemistry* **2008**, *40* (2), 528–536. https://doi.org/10.1016/j.soilbio.2007.09.021.
(46) Gruseck, R.; Hofmann, T.; Zumstein, M. Flavonoid Stability and Biotransformation in Agricultural Soils: Effects of Hydroxylation, Methoxylation, and Glycosylation. *J. Agric. Food Chem.* **2025**, *73* (23), 14245–14252. https://doi.org/10.1021/acs.jafc.5c02814.
(47) Bao, L.; Liu, Y.; Ding, Y.; Shang, J.; Wei, Y.; Tan, Y.; Zi, F. Interactions Between Phenolic Acids and Microorganisms in Rhizospheric Soil From Continuous Cropping of Panax Notoginseng. *Front. Microbiol.* **2022**, *13*, 791603. https://doi.org/10.3389/fmicb.2022.791603.
(48) Zwetsloot, M. J.; Ucros, J. M.; Wickings, K.; Wilhelm, R. C.; Sparks, J.; Buckley, D. H.; Bauerle, T. L. Prevalent Root-Derived Phenolics Drive Shifts in Microbial Community Composition and Prime Decomposition in Forest Soil. *Soil Biology and Biochemistry* **2020**, *145*, 107797. https://doi.org/10.1016/j.soilbio.2020.107797.
(49) Dabetic, N.; Todorovic, V.; Malenovic, A.; Sobajic, S.; Markovic, B. Optimization of Extraction and HPLC–MS/MS Profiling of Phenolic Compounds from Red Grape Seed Extracts Using Conventional and Deep Eutectic Solvents. **2022**.
(50) Andersen, I. K. L.; Laursen, B. B.; Rasmussen, J.; Fomsgaard, I. S. Optimised Extraction and LC-MS/MS Analysis of Flavonoids Reveal Large Field Variation in Exudation into Lupinus Angustifolius L. Rhizosphere Soil. *Rhizosphere* **2022**, *22*, 100516. https://doi.org/10.1016/j.rhisph.2022.100516.

(51) Zhang, J.-Y.; Wang, Z.-J.; Zhang, Q.; Wang, F.; Ma, Q.; Lin, Z.-Z.; Lu, J.-Q.; Qiao, Y.-J. Rapid Screening and Identification of Target Constituents Using Full Scan-Parent Ions List-Dynamic Exclusion Acquisition Coupled to Diagnostic Product Ions Analysis on a Hybrid LTQ-Orbitrap Mass Spectrometer. *Talanta* **2014**, *124*, 111–122. https://doi.org/10.1016/j.talanta.2013.11.025.
(52) Xing, T. T.; Zhao, X. J.; Zhang, Y. D.; Li, Y. F. Fast Separation and Sensitive Quantitation of Polymethoxylated Flavonoids in the Peels of *Citrus* Using UPLC-Q-TOF-MS. *J. Agric. Food Chem.* **2017**, *65* (12), 2615–2627. https://doi.org/10.1021/acs.jafc.6b05821.
(53) Khan, M. K.; Abert-Vian, M.; Fabiano-Tixier, A.-S.; Dangles, O.; Chemat, F. Ultrasound-Assisted Extraction of Polyphenols (Flavanone Glycosides) from Orange (Citrus Sinensis L.) Peel. *Food Chemistry* **2010**, *119* (2), 851–858. https://doi.org/10.1016/j.foodchem.2009.08.046.
(54) Okubo, M.; Minami, H.; Yamamoto, Y. Penetrationrrelease Behaviors of Various Solvents Intorfrom Micron-Sized Monodispersed Hollow Polymer Particles ଌ. **1999**.
(55) *Seasonality of Fresh Orange*. TRIDGE. https://www.tridge.com/intelligences/orange/season (accessed 2025-06-10).
(56) Kawaii, S.; Tomono, Y.; Katase, E.; Ogawa, K.; Yano, M. Quantitation of Flavonoid Constituents in *Citrus* Fruits. *J. Agric. Food Chem.* **1999**, *47* (9), 3565–3571. https://doi.org/10.1021/jf990153+.
(57) Multari, S.; Licciardello, C.; Caruso, M.; Anesi, A.; Martens, S. Flavedo and Albedo of Five Citrus Fruits from Southern Italy: Physicochemical Characteristics and Enzyme-Assisted Extraction of Phenolic Compounds. *Food Measure* **2021**, *15* (2), 1754–1762. https://doi.org/10.1007/s11694-020-00787-5.
(58) Sawalha, S. M. S.; Arráez-Román, D.; Segura-Carretero, A.; Fernández-Gutiérrez, A. Quantification of Main Phenolic Compounds in Sweet and Bitter Orange Peel Using CE–MS/MS. *Food Chemistry* **2009**, *116* (2), 567–574. https://doi.org/10.1016/j.foodchem.2009.03.003.
(59) Golgeri M, D. B.; Mulla, S. I.; Bagewadi, Z. K.; Faniband, B.; Mishra, P.; Bankole, P. O.; Sharma, S.; Américo-Pinheiro, J. H. P.; Bharagava, R. N.; Romanholo Ferreira, L. F. Microbial Naringinase: From Microbial Source to Its Current Applications in Various Fields. *Biologia* **2025**. https://doi.org/10.1007/s11756-025-01888-6.
(60) Luo, L.; Cui, Y.; Zhang, S.; Li, L.; Li, Y.; Zhou, P.; Sun, B. Preparative Separation of Grape Skin Polyphenols by High-Speed Counter-Current Chromatography. *Food Chemistry* **2016**, *212*, 712–721. https://doi.org/10.1016/j.foodchem.2016.06.009.

Supplementary Information

Table SI 2: *Orange Origin: The table provides an overview of all orange batches used in this study. The Batch ID represents a short identifier used throughout the study. Information on origin and if oranges were labeled as organically or conventionally is based on labeling provided on the original packaging at the time of purchase. The storage duration was estimated by taking into account the date of purchase and the typical harvest periods, as reported by TRIDGE[55])*

Batch ID	Description	Purchase Date	Harvest Season	Estimated Storage Period
O.SAf	Organic Valencia Oranges (Billa, S. Africa)	08.10.2024	High season: Jul-Sep Low season: Jun-Oct	~ Freshly harvested or short storage.
O.GR	Organic Valecia Oranges (Greece)	21.10.2024	High season: Dec-Jan Low season: Nov-Feb	~ Some months post-harvest storage (export).
C.SAf	Conventional Oranges (San Lucar, S. Africa)	21.10.2024	High season: Jul-Sep Low season: Jun-Oct	~ Freshly harvested or short storage.
C.BO	Conventional Oranges (Hofer, Botswana)	16.10.2024	probably like South Africa (same climate zone) but N/A	~ Freshly harvested or short storage.
O.NA	Organic Oranges (Lidl, Origin N/A)	26.09.2024	N/A	~ Unknown.

O.IT	Organic Navel Oranges, (Billa, Italy)	23.01.2025	High season: Nov-Dec	~ Some weeks post-harvest storage.

Figure SI 1: *Photo of peeled orange peel as an example of peeling accuracy. Flavedo and albedo layers were separated together from the edible parts, with no pulp included, before further processing.*

Table SI 3: *Orange weight: Prior to processing, the average fresh peel content of an orange was determined to be 24.6 ± 4.5% of the total fruit weight. Of this fresh peel, 28.9 ± 4.3% accounted for dried peel. This corresponds to an average of 7.2 ± 2.0% dry peel per orange.*

Batch	Replicate	whole orange [g]	fresh peel [g]	fresh peel [% of whole orange]	dry peel [g]	dry peel [% of fresh peel]	dry peel [% of whole orange]
organic-Lidl oranges country NA - Powder 26.9.24	orange 1	233.4	48.8	20.9	12.1	24.9	5.2
	orange 2	209.4	38.6	18.4	9.8	25.5	4.7
	orange 3	189.2	46.5	24.6	11.9	25.7	6.3
organic-Billa Valencia oranges SouthAfrica - Powder 8.10	orange 1	170.5	42.3	24.8	15.2	35.8	8.9
	orange 2	166.9	49.0	29.4	15.2	31.0	9.1
	orange 3	175.8	51.9	29.5	15.8	30.5	9.0

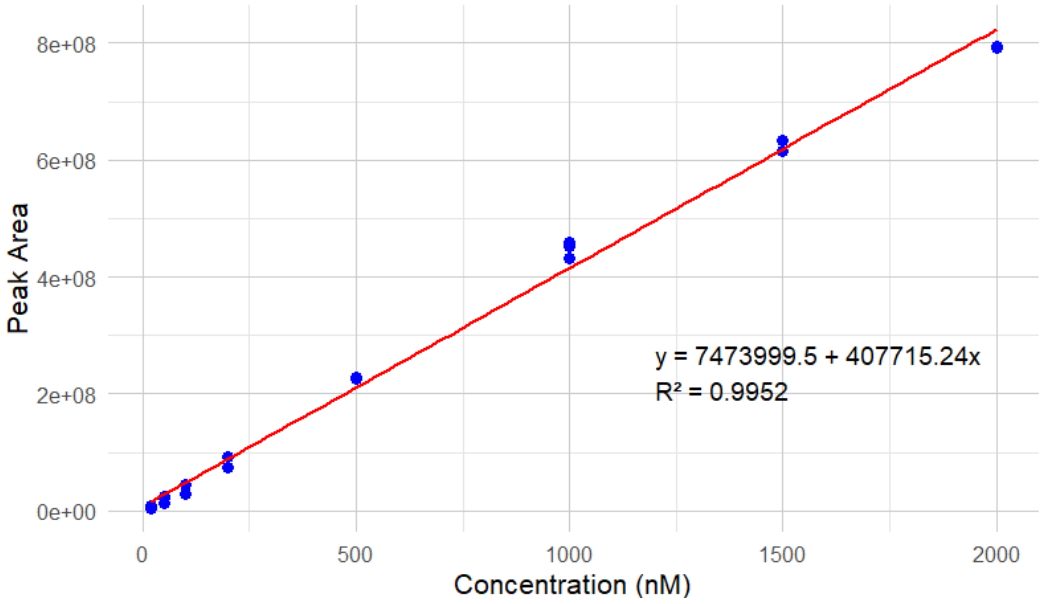

Figure SI 2: Calibration curve for naringin (part 1): The calibration was performed using a naringin standard measured via UHPLC-HRMS. Peak area was plotted against concentration (nM), and a linear regression model was applied. Each concentration point (20, 50, 100, 200, 500, 1000, 1500, 2000 nM) was measured in duplicate and used to generate the calibration curve.

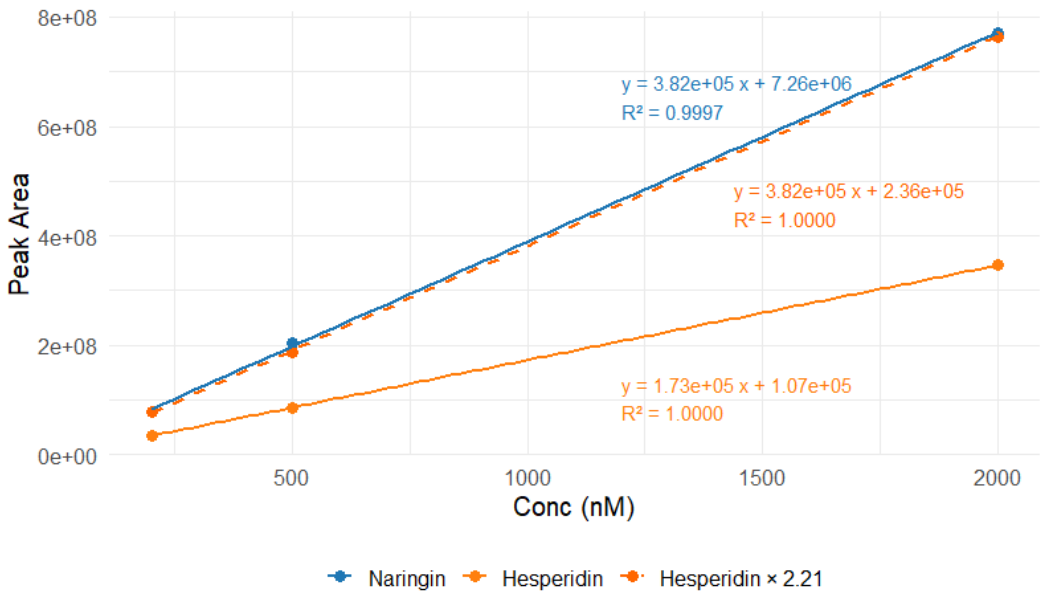

Figure SI 3: *Comparison of peak area to concentration relationship for naringin and hesperidin: Calibration curves were generated via UHPLC-HRMS for naringin (orange) and hesperidin (blue), showing a significantly lower peak area for hesperidin at equal concentrations. This leads to a strong underestimation of hesperidin concentrations when using the naringin calibration curve. To account for this discrepancy, hesperidin values were retrospectively adjusted by a factor of 2.21 (green), resulting in comparable linear behavior across the measured concentration range.*

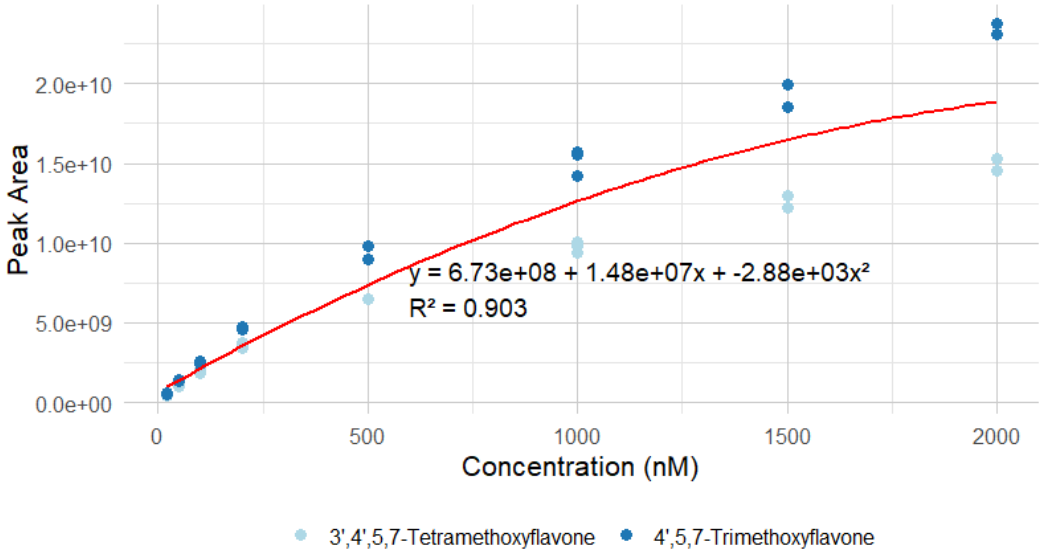

Figure SI 4: *A shared calibration curve for all PMFs (part 1) was generated using the combined response of the standards 4',5,7-Trimethoxyflavone and 3',4',5,7-Tetramethoxyflavone, measured via UHPLC-HRMS. For each concentration (20, 50, 100, 200, 500, 1000, 1500, 2000 nM), two to three replicate injections per standard were recorded, resulting in multiple data points per concentration. Peak area was plotted against concentration, and a quadratic regression model was applied.*

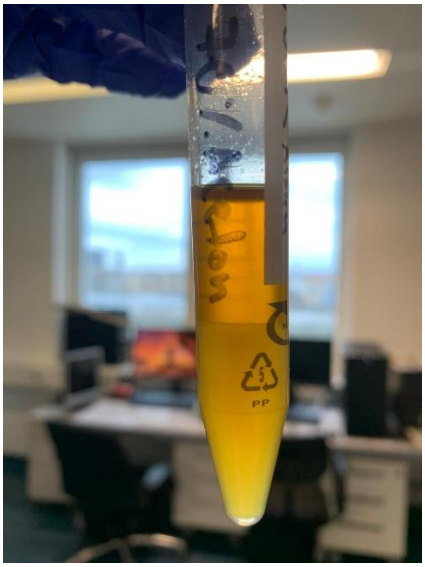

Figure SI 5: *12-fold concentrated stock solution used for soil incubation experiments: The solution consistently showed rapid phase separation into two roughly equal layers: a transparent dark yellow upper phase and a turbid light yellow lower phase. Prior to each soil inoculation, the stock was vortexed thoroughly to ensure homogeneity.*

***Table SI 4**: Rehydration (1): amount of ultra-pure water (in ml) that was re-added to both autoclaved and active soil incubation samples after one week, based on weight loss due to evaporation. Water loss was determined gravimetrically, and the equivalent volume of water was replenished accordingly. Sample ID indicates the intended number of days (d) from T0 at which the sample was scheduled for measurement. Samples labeled with x or m denote replacement samples. The table includes mean and standard deviation of the added volumes for active and autoclaved samples separately.*

after 1 week			
Sample ID autoclaved	**Addition water [ml]**	**Sample ID active**	**Addition water [ml]**
10d (1)	6	**10d (1)**	8
10d (2)	3	**10d (2)**	3
10d (3)	3	**10d (3)**	2
13d (1)	2	**13d (1)**	6
13d (2)	4	**13d (2)**	3
13d (3)	0	**13d (3)**	5
17d (1)	1	**17d (1)**	10
17d (2)	1	**17d (2)**	5
17d (3)	0	**17d (3)**	9
20d (1)	0	**20d (1)**	7
20d (2)	2	**20d (2)**	5
20d (3)	8	**20d (3)**	5
x1	1	**x2**	6
x2	2	**x3**	4
x3	4	**m1**	10
		m2	5
mean	2.5	**mean**	5.8
SD	2.3	**SD**	2.4

Table SI 5: *Rehydration (2): amount of ultra-pure water (in ml) that was re-added to both autoclaved and active soil incubation samples after two weeks, based on weight loss due to evaporation. Water loss was determined gravimetrically, and the equivalent volume of water was replenished accordingly. Sample ID indicates the intended number of days (d) from T0 at which the sample was scheduled for measurement. Samples labeled with x or m denote replacement samples. The table includes mean and standard deviation of the added volumes for active and autoclaved samples separately.*

after 2 weeks			
Sample ID autoclaved	**Addition water [ml]**	**Sample ID active**	**Addition water [ml]**
17d (1)	5	**17d (1)**	13
17d (2)	2	**17d (2)**	2
17d (3)	4	**17d (3)**	4
20d (1)	5	**20d (1)**	8
20d (2)	6	**20d (2)**	5
20d (3)	5	**20d (3)**	5
x1	5	**x2**	4
x2	4	**x3**	4
x3	4	**m1**	4
		m2	4
mean	4.4	**mean**	5.3
SD	1.1	**SD**	3.1

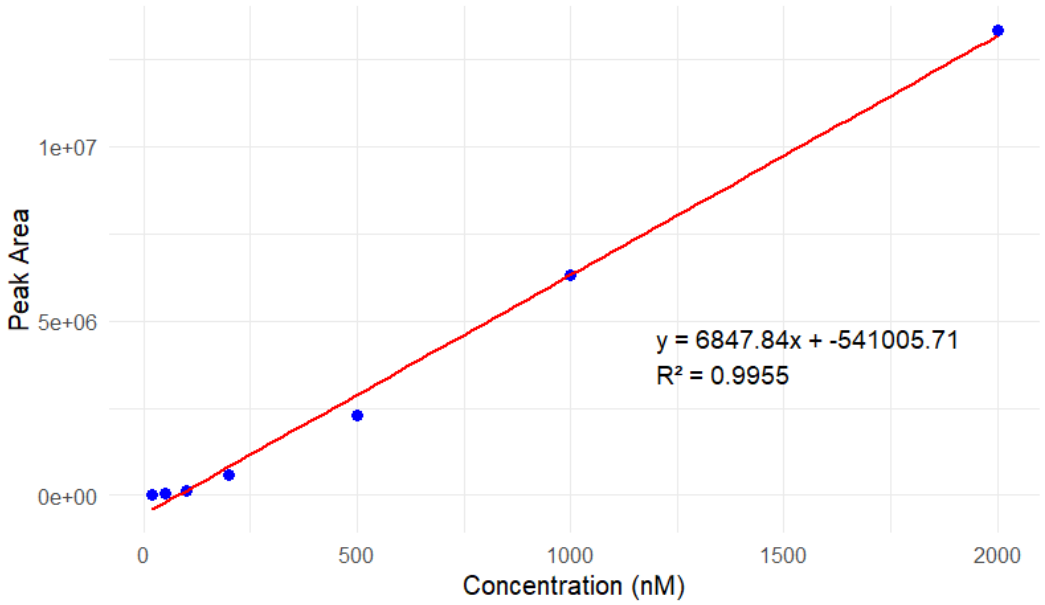

Figure SI 6: *Calibration curve for naringin (part 2): The calibration was performed using a naringin standard measured via UHPLC-HRMS. Peak area was plotted against concentration (nM), and a linear regression model was applied. Each concentration point (20, 50, 100, 200, 500, 1000, 2000 nM) was measured without replicates and used to generate the calibration curve.*

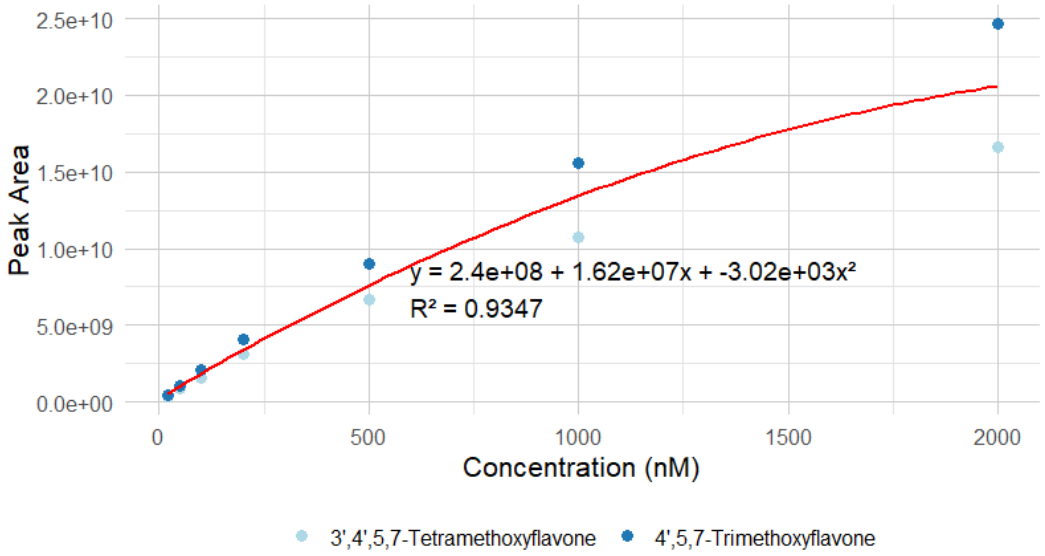

Figure SI 7: *A shared calibration curve for all PMFs (part 2: soil incubation) was generated using single measurements of the standards 4',5,7-Trimethoxyflavone and 3',4',5,7-Tetramethoxyflavone at each concentration (20, 50, 100, 200, 500, 1000, 2000 nM), measured via UHPLC-HRMS. The individual responses were combined, and peak area was plotted against concentration. A quadratic regression model was applied.*

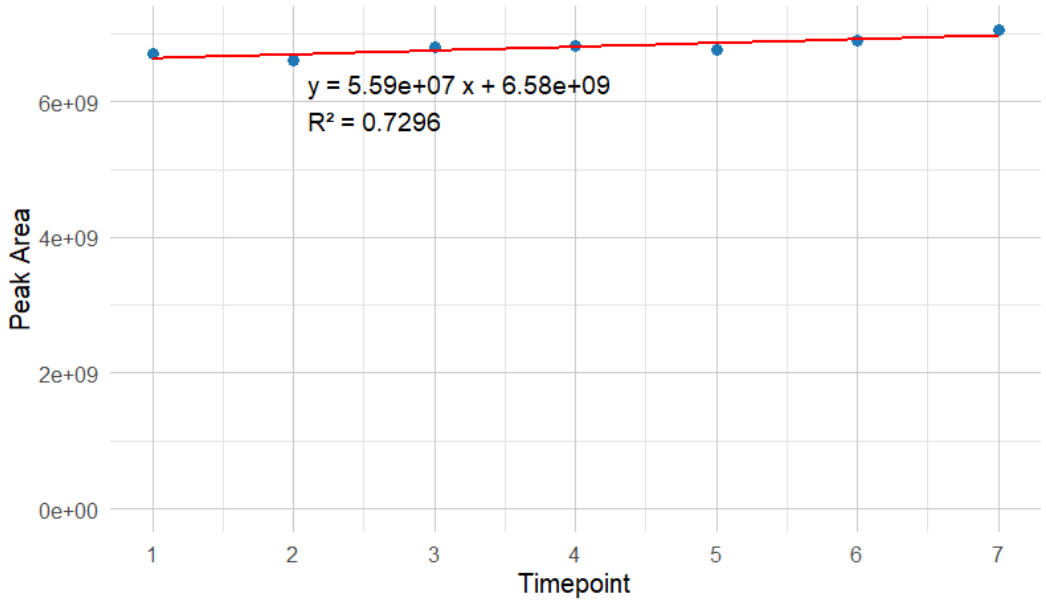

Figure SI 8: *Instrument signal stability during long-term UHPLC-HRMS soil incubation analysis: To monitor potential signal drift over time, a 500 nM standard of 3',4',5,7-Tetramethoxyflavone was repeatedly measured (n = 7) across the full run of the soil incubation samples. The observed fluctuations in peak area remained within the expected range of instrumental variability and did not indicate any systematic drift. Therefore, no correction of sample data was necessary.*

Table SI 6: *Flavonoid reference standards for targeted UHPLC-HRMS screening: Compounds include aglycones, glycoylated, and methoxylated flavonoids. All standards were used for the identification of compounds in citrus peel extracts.*

Molecule Name	Molecular Formula	Precursor m/z	Precursor Adduct	Precursor Charge	Explicit Retention Time
Catechin	$C_{15}H_{14}O_6$	289.071761 7	M-H	-1	2.1
Kaempferol	$C_{15}H_{10}O_6$	285.040461 6	M-H	-1	10.8
Luteolin	$C_{15}H_{10}O_6$	285.040461 6	M-H	-1	10.2
Naringenin	$C_{15}H_{12}O_5$	271.061197	M-H	-1	10.45

Genistein	$C_{15}H_{10}O_5$	269.045547	M-H	-1	10.5
Apigenin	$C_{15}H_{10}O_5$	269.045547	M-H	-1	11.2
Rutin	$C_{27}H_{30}O_{16}$	609.1461084	M-H	-1	7.8
Naringin	$C_{27}H_{32}O_{14}$	579.1719293	M-H	-1	8.5
Quercetin	$C_{15}H_{10}O_7$	301.0353762	M-H	-1	9.8
Myricetin	$C_{15}H_{10}O_8$	317.0302908	M-H	-1	8.6
Hesperetin	$C_{16}H_{14}O_6$	301.0717617	M-H	-1	10.7
Q-BZF	$C_{15}H_{10}O_8$	317.0302908	M-H	-1	4.8
K-BZF	$C_{15}H_{10}O_7$	301.0353762	M-H	-1	6.6
M-BZF	$C_{15}H_{10}O9$	333.0252054	M-H	-1	2.4
Chrysoeriol (neg)	$C_{16}H_{12}O_6$	299.05611	M-H	-1	11.2
Chrysoeriol (pos)	$C_{16}H_{12}O_6$	301.07066	M+H	1	11.2
3′,4′,5,7-Tetramethoxyflavone	$C_{19}H_{18}O_6$	343.11761	M+H	1	11.7
4′,5,7-Trimethoxyflavone	$C_{18}H_{16}O_5$	313.10705	M+H	1	12.4

Kaempferol-3-O-glucoside	$C_{21}H_{20}O_{11}$	447.093285	M-H	-1	8.7
Apigenin-7-O-glucoside	$C_{21}H_{20}O_{10}$	431.09837	M-H	-1	8.9
Genkwanin	$C_{16}H_{12}O_5$	283.061197	M-H	-1	12.7

Table SI 7: *Selected PMFs searched for in citrus peel extracts based on the theoretical m/z values reported by Zhang et al.[51]. Exact mass-to-charge ratios (m/z) were used to assign compounds to peaks in the chromatograms, with corresponding retention times. No reference standards were available for these PMFs; identifications are based solely on the precursor ion masses.*

Substituents	Molecular Formula	Precursor m/z	Precursor Adduct	Precursor Charge	RT
2OCH3	$C_{17}H_{14}O_4$	283.09649	M+H	1	-
2OCH3	$C_{17}H_{16}O_4$	285.11214	M+H	1	-
2OCH3+OH	$C_{17}H_{14}O_5$	299.0914	M+H	1	-
2OCH3+OH	$C_{17}H_{16}O_5$	301.10705	M+H	1	-
3OCH3	$C_{18}H_{16}O_5$	313.107055	M+H	1	-
3OCH3	$C_{18}H_{18}O_5$	315.08629	M+H	1	-
2OCH3+2OH	$C_{17}H_{14}O_6$	315.122705	M+H	1	-
2OCH3+2OH	$C_{17}H_{16}O_6$	317.10194	M+H	1	-
3OCH3+OH	$C_{18}H_{16}O_6$	329.101955	M+H	1	-

3OCH3+OH	$C_{18}H_{18}O_6$	331.08119	M+H	1	-
2OCH3+3OH	$C_{17}H_{14}O_7$	331.117605	M+H	1	-
2OCH3+3OH	$C_{17}H_{16}O_7$	333.09684	M+H	1	-
4OCH3	$C_{19}H_{18}O_6$	343.11762	M+H	1	11.99, 12.24
4OCH3	$C_{19}H_{20}O_6$	345.096855	M+H	1	-
3OCH3+2OH	$C_{18}H_{16}O_7$	345.13327	M+H	1	-
3OCH3+2OH	$C_{18}H_{18}O_7$	347.07609	M+H	1	-
2OCH3+4OH	$C_{17}H_{14}O_8$	347.112505	M+H	1	-
2OCH3+4OH	$C_{17}H_{16}O_8$	349.09174	M+H	1	-
4OCH3+OH	$C_{19}H_{18}O_7$	359.11252	M+H	1	-
4OCH3+OH	$C_{19}H_{20}O_7$	361.091755	M+H	1	-
3OCH3+3OH	$C_{18}H_{16}O_8$	361.12817	M+H	1	-
3OCH3+3OH	$C_{18}H_{18}O_8$	363.07099	M+H	1	-
2OCH3+5OH	$C_{17}H_{14}O_9$	363.107405	M+H	1	-
2OCH3+5OH	$C_{17}H_{16}O_9$	365.08664	M+H	1	-
5OCH3	$C_{20}H_{20}O_7$	373.128185	M+H	1	11.33, 11.58, 12.92
5OCH3	$C_{20}H_{22}O_7$	375.10742	M+H	1	-

4OCH3+2OH	$C_{19}H_{18}O_8$	375.143835	M+H	1	-
4OCH3+2OH	$C_{19}H_{20}O_8$	377.086655	M+H	1	-
3OCH+4OH	$C_{18}H_{16}O_9$	377.12307	M+H	1	-
3OCH+4OH	$C_{18}H_{18}O_9$	379.102305	M+H	1	-
5OCH3+OH	$C_{20}H_{20}O_8$	389.123085	M+H	1	-
5OCH3+OH	$C_{20}H_{22}O_8$	391.10232	M+H	1	-
4OCH3+3OH	$C_{19}H_{18}O_9$	391.138735	M+H	1	-
4OCH3+3OH	$C_{19}H_{20}O_9$	393.11797	M+H	1	-
6OCH3	$C_{21}H_{22}O_8$	403.13875	M+H	1	8.32, 9.39, 13.76
6OCH3	$C_{21}H_{24}O_8$	405.117985	M+H	1	-
5OCH3+2OH	$C_{20}H_{20}O_9$	405.1544	M+H	1	-
5OCH3+2OH	$C_{20}H_{22}O_9$	407.133635	M+H	1	-
6OCH3+OH	$C_{21}H_{22}O_9$	419.13365	M+H	1	-
6OCH3+OH	$C_{21}H_{24}O_9$	421.1493	M+H	1	-
7OCH3	$C_{22}H_{24}O_9$	433.149315	M+H	1	12.62
7OCH3	$C_{22}H_{26}O_9$	435.164965	M+H	1	-

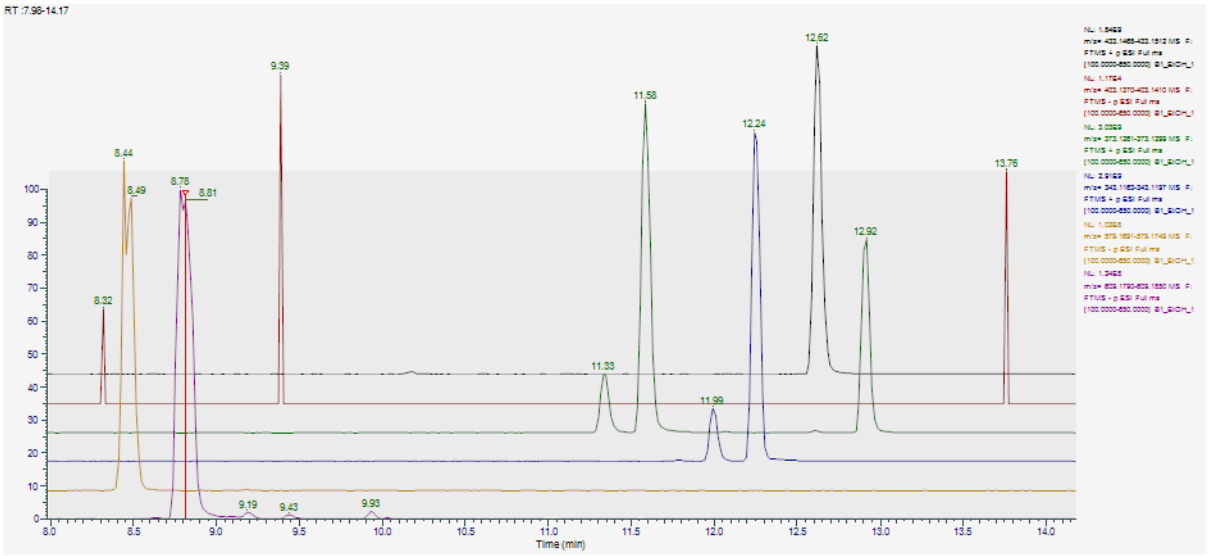

Figure SI 9: *Extract from the HPLC-HRMS chromatogram showing detected peaks of the analyzed compounds. The following mass signals were detected: m/z 433.1469 (RT 12.62 min, black) – PMF with 7OCH₃, m/z 403.1370 (RT 8.32, 9.39, 13.76 min, red) – PMFs with 6OCH₃, m/z 373.1262 (RT 11.33, 11.58, 12.92 min, green) – PMFs with 5OCH₃, m/z 343.1163 (RT 11.99, 12.24 min, blue) – PMFs with 4OCH₃, m/z 579.1691 (RT 8.44–8.49 min, yellow) – Naringin, m/z 609.1790 (RT 8.78–8.81 min, purple) – Hesperidin*

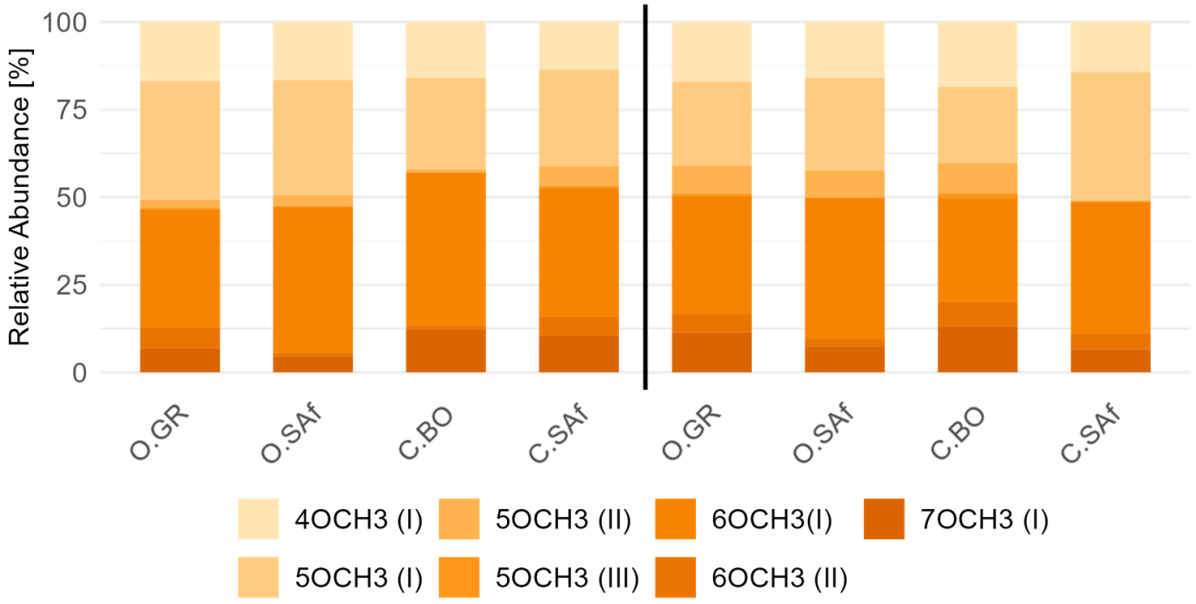

Figure SI 10*: Relative abundance of PMFs in citrus peel extracts normalized to 100%. This figure corresponds to Figure 7 but shows normalized peak intensities instead of absolute values, allowing better visualization of the relative proportions of individual PMFs.*

Table SI 8: *Absolute concentrations of hesperidin, naringin, and PMFs, as well as the total flavonoid content, extracted from orange peel samples derived from organically and conventionally grown oranges originating from Botswana, Greece, and South Africa. Extractions were performed using two solvents: ChCl/U20 and EtOH60 with a fixed S/L ratio of 1:10. The mean yield for total flavonoids was 11.70 mg/gDW for ChCl/U20 and 13.12 mg/gDW for EtOH60.*

Group	Solvent	Hesperidin [mg/gDW]	Hesperidin SD [mg/gDW]	Naringin [mg/gDW]	Naringin SD [mg/gDW]	PMFs [mg/gDW]	PMFs SD [mg/gDW]	Total [mg/gDW]	Total SD [mg/gDW]
O.GR	ChCl/U20	13.07	0.47	0.41	0.03	1.19	0.10	14.66	0.57
O.GR	EtOH60	11.26	0.18	0.39	0.02	2.02	0.15	13.67	0.24
O.SAf	ChCl/U20	14.70	0.21	0.62	0.01	0.76	0.07	16.08	0.22
O.SAf	EtOH60	8.08	0.17	0.53	0.02	1.18	0.10	9.8	0.12
C.BO	ChCl/U20	3.46	1.30	0.13	0.09	0.32	0.03	3.91	1.47
C.BO	EtOH60	10.94	1.04	0.96	0.30	2.89	0.20	14.79	1.26
C.SAf	ChCl/U20	9.66	0.35	1.13	0.05	1.34	0.11	12.14	0.43
C.SAf	EtOH60	12.48	0.05	1.02	0.06	0.70	0.06	14.2	0.11

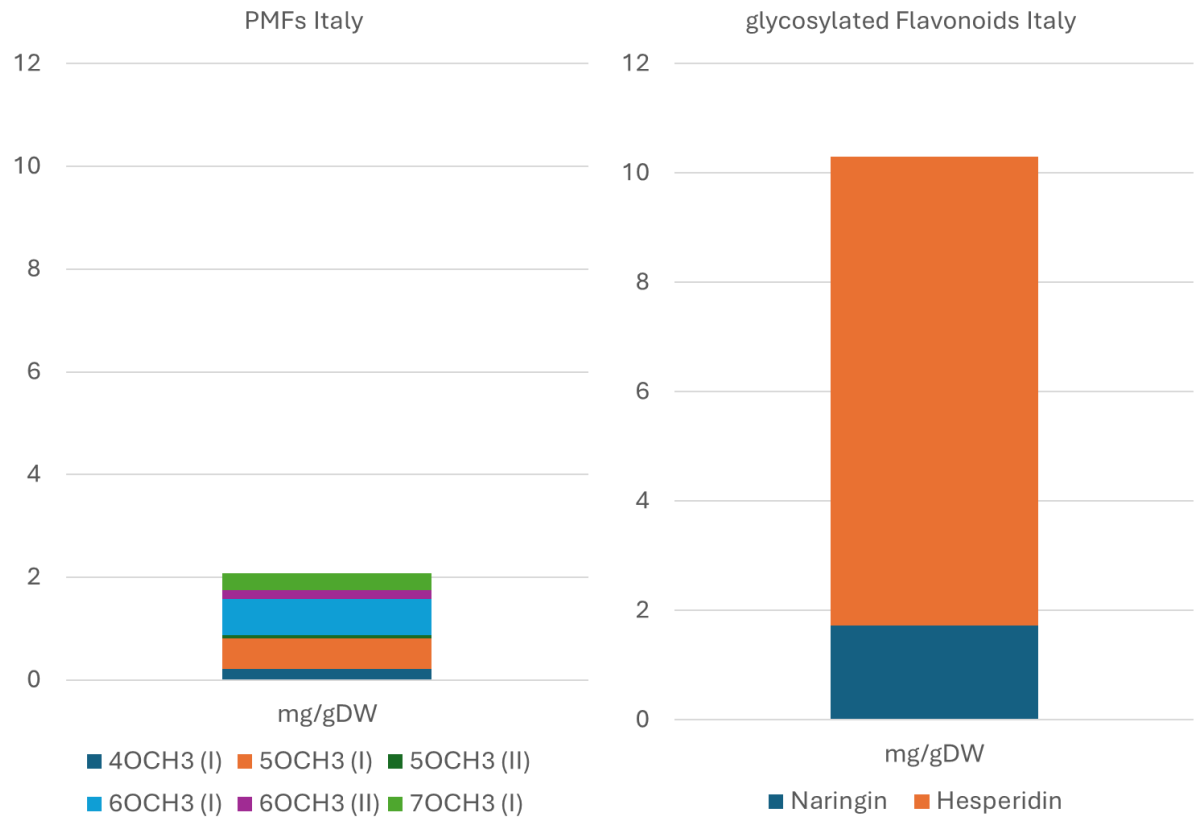

Figure SI 11: *The flavonoid content (mg/g DW) was determined in the stock solution used for soil incubation before the 12-fold concentration. This quantification was carried out to enable adjustment of the concentration so that a minimum of 0.5 nM per PMF would be reached after up-concentration. The graphs show both PMFs and glycosylated flavonoids detected in the orange O.IT extract prior to concentration.*

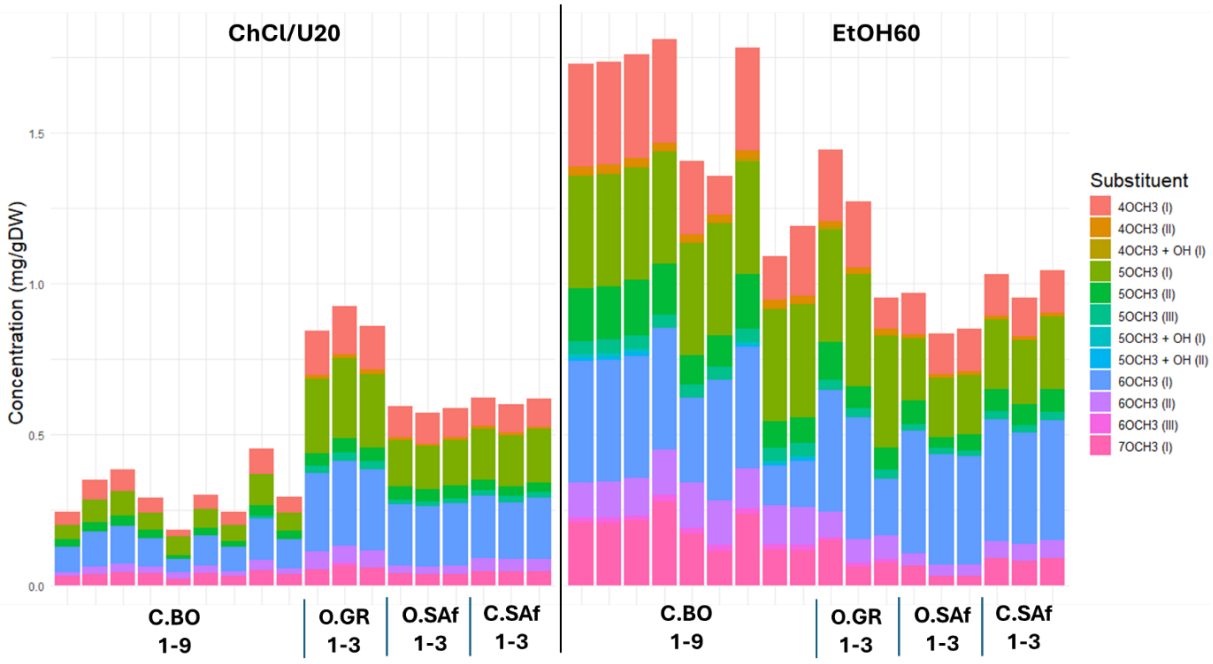

Figure SI 12: *Concentrations of individual PMFs (mg/g dry weight) detected in citrus peel extracts at a lower dilution factor (1:20). No mean values were calculated from triplicates or from the nine samples per batch (1-3/9). This figure highlights that, in contrast to the 1:250 dilution used for quantification, small amounts of PMFs hydroxylated with a single OH group are still detectable at 1:20 dilution. At higher dilution, only fully methoxylated PMFs were observed.*

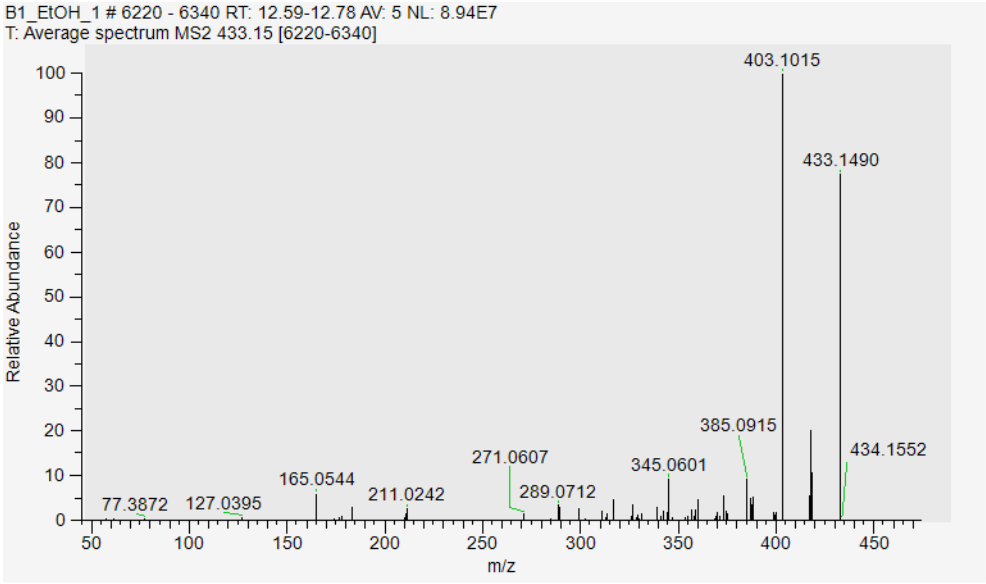

***Figure SI 13**: MS² spectrum of PMF substituted with 7OCH3 (I) (precursor m/z 433.15). The dominant fragment at m/z 403.1015 corresponds to the loss of two OMe. Other fragments, such as those at m/z 418.125 and 387.067, are present in the spectrum but not labeled due to limited space in the figure.*

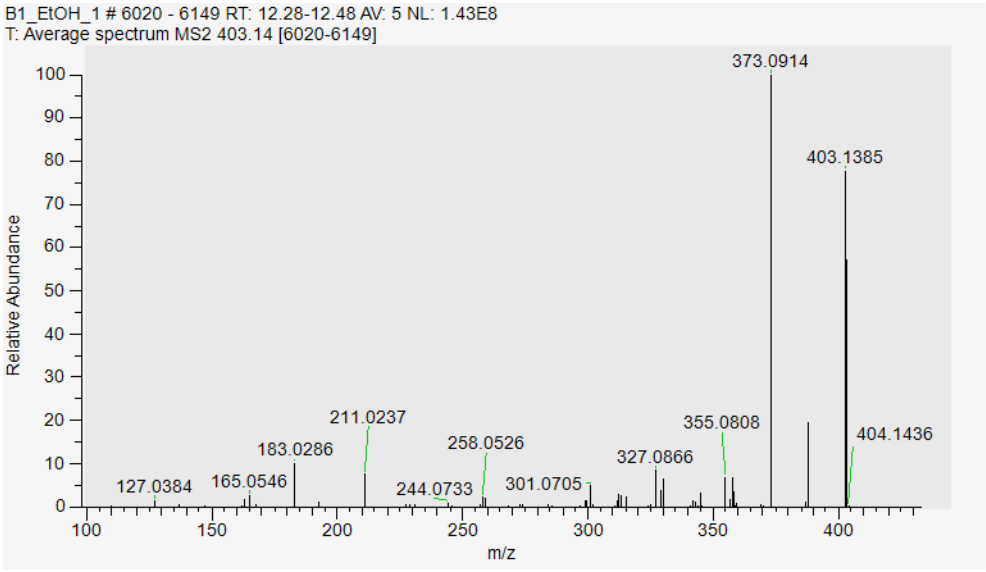

***Figure SI 14:** MS² spectrum of PMF substituted with 6OCH3 (I) (precursor m/z 403.16). The dominant fragment at m/z 373.0914 corresponds to the loss of two OMe. Other fragments, such as those at m/z 388.115, 358.068 and 330.073 are present in the spectrum but not labeled due to limited space in the figure.*

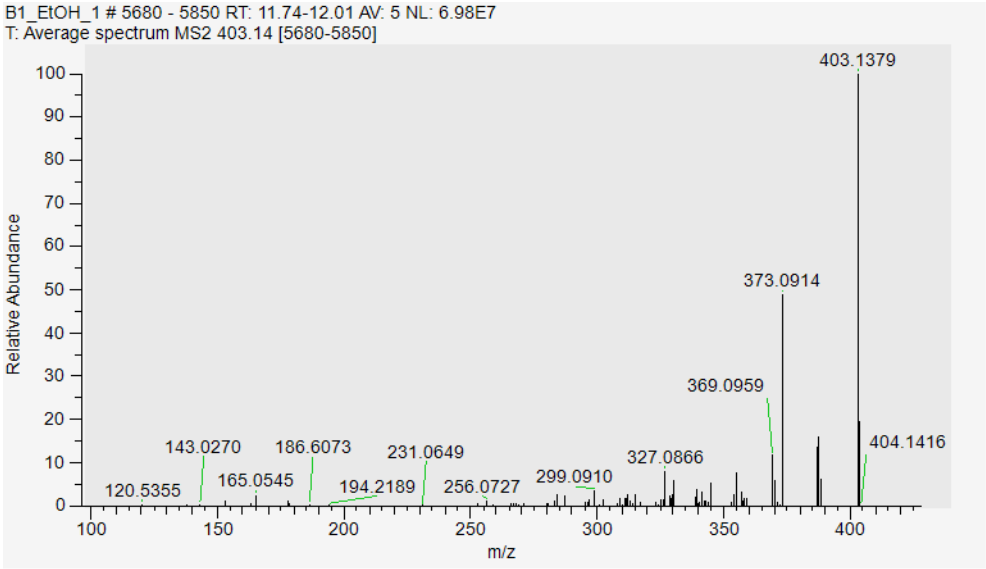

Figure SI 15: *MS² spectrum of PMF substituted with 6OCH3 (II) (precursor m/z 403.16). The dominant fragment at m/z 373.0914 corresponds to the loss of two OMe. Other fragments, such as those at m/z 387.107, 388.115 and 355.078 are present in the spectrum but not labeled due to limited space in the figure.*

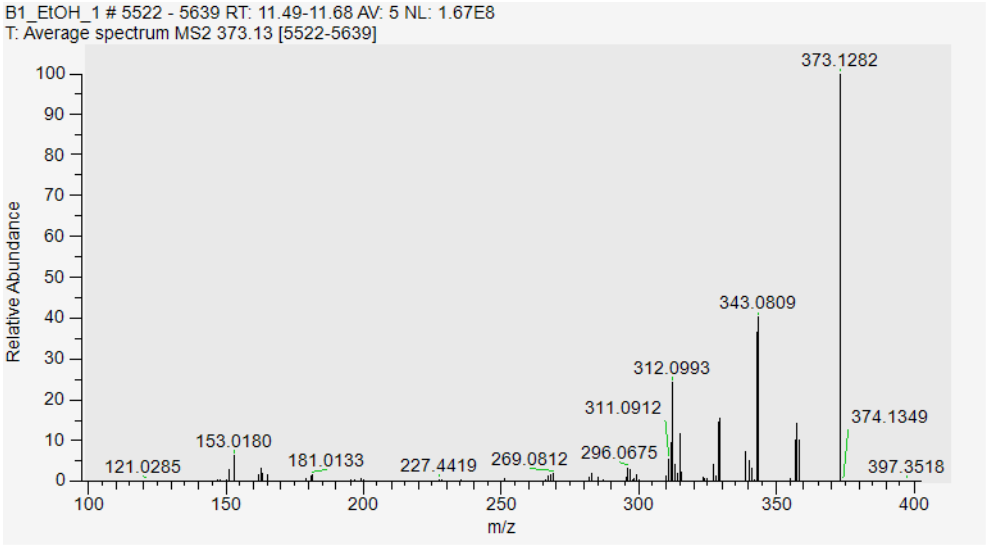

Figure SI 16: *MS² spectrum of PMF substituted with 5OCH3 (I) (precursor m/z 373.13). The dominant fragment at m/z 343.0809 corresponds to the loss of two OMe. Other fragments, such as those at m/z 357.097, 358.104, 329.102 and 339.086 are present in the spectrum but not labeled due to limited space in the figure.*

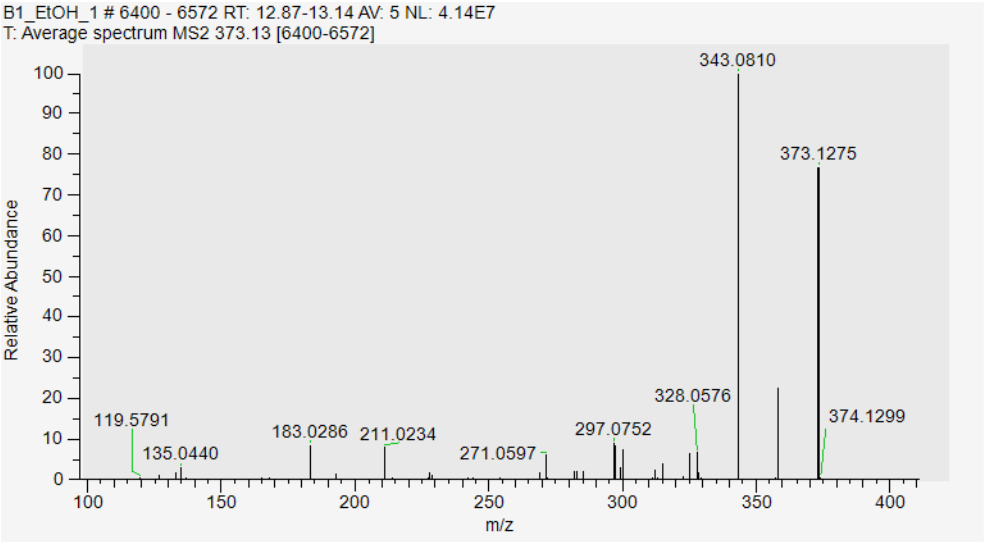

Figure SI 17: *MS² spectrum of PMF substituted with 5OCH3 (II) (precursor m/z 373.13). The dominant fragment at m/z 343.0809 corresponds to the loss of two OMe. Other fragments, such as those at m/z 358.104, 325.070 and 315.086 are present in the spectrum but not labeled due to limited space in the figure.*

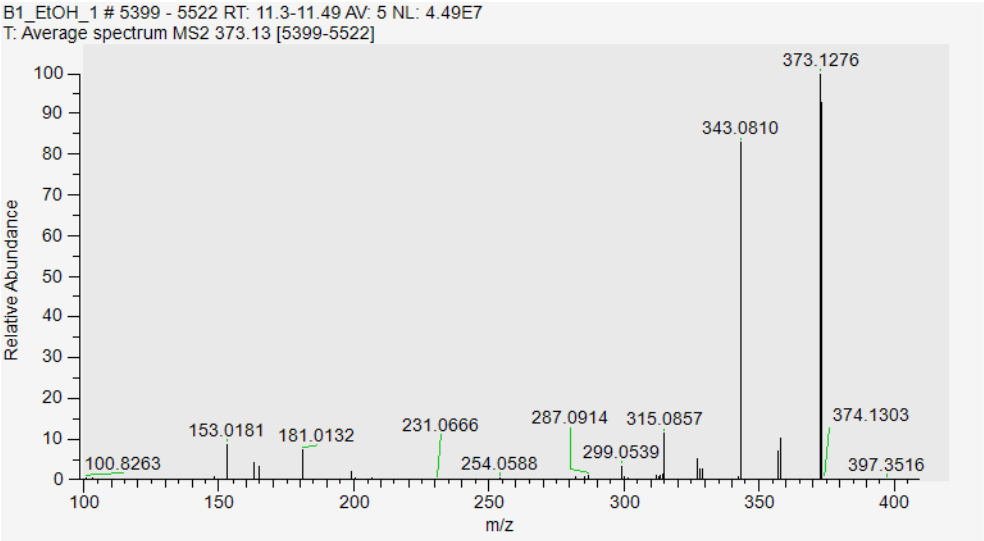

Figure SI 18: *MS² spectrum of PMF substituted with 5OCH3 (III) (precursor m/z 373.13). The dominant fragment at m/z 343.0809 corresponds to the loss of two OMe. Other fragments, such as those at m/z 358.104, 357.096, 329.101 and 327.049 are present in the spectrum but not labeled due to limited space in the figure.*

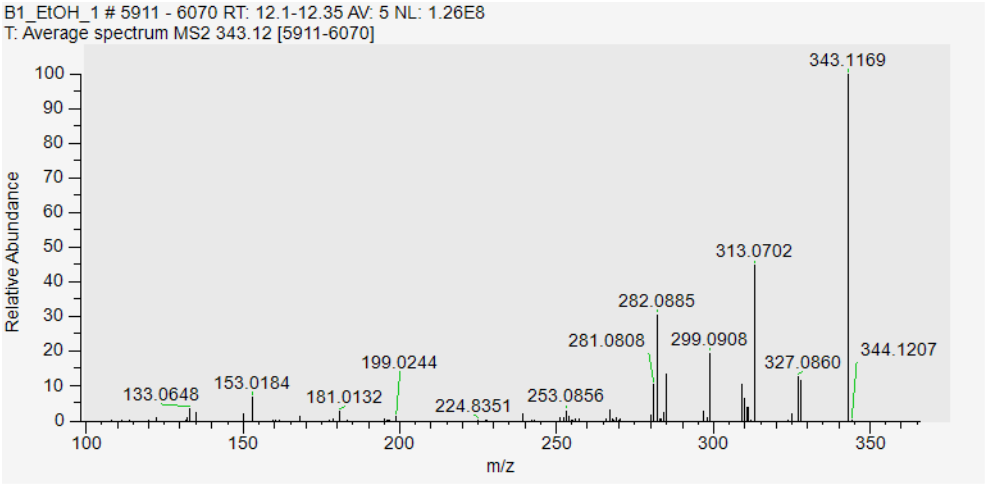

Figure SI 19: *MS² spectrum of PMF substituted with 4OCH3 (I) (precursor m/z 343.12). The dominant fragment at m/z 313.0702 corresponds to the loss of two OMe. Other fragments, such as those at m/z 328.093, 309.075, 310.083 and 285.076are present in the spectrum but not labeled due to limited space in the figure.*

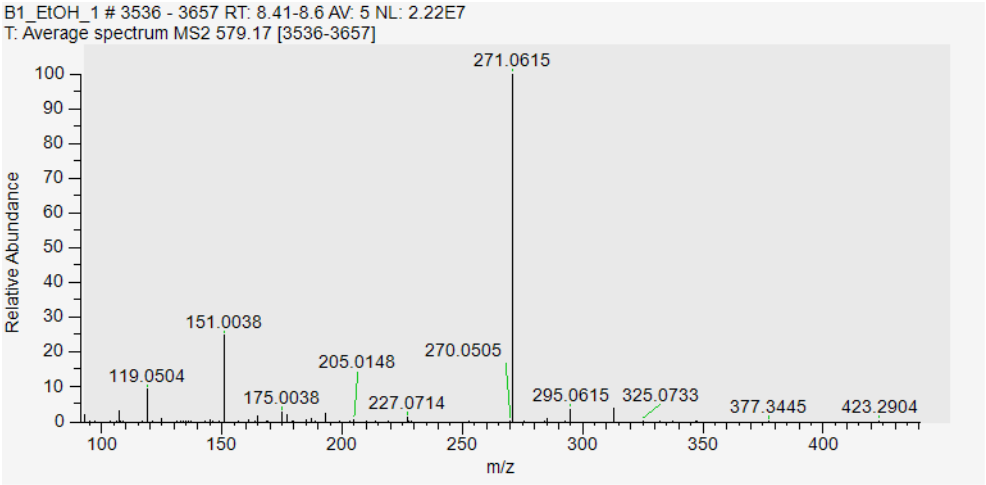

Figure SI 20: *MS² spectrum of naringin (precursor m/z 579.17). The spectrum shows characteristic losses of glucose and rhamnose, resulting in a prominent fragment at m/z 271.0615, corresponding to the aglycone naringenin.*

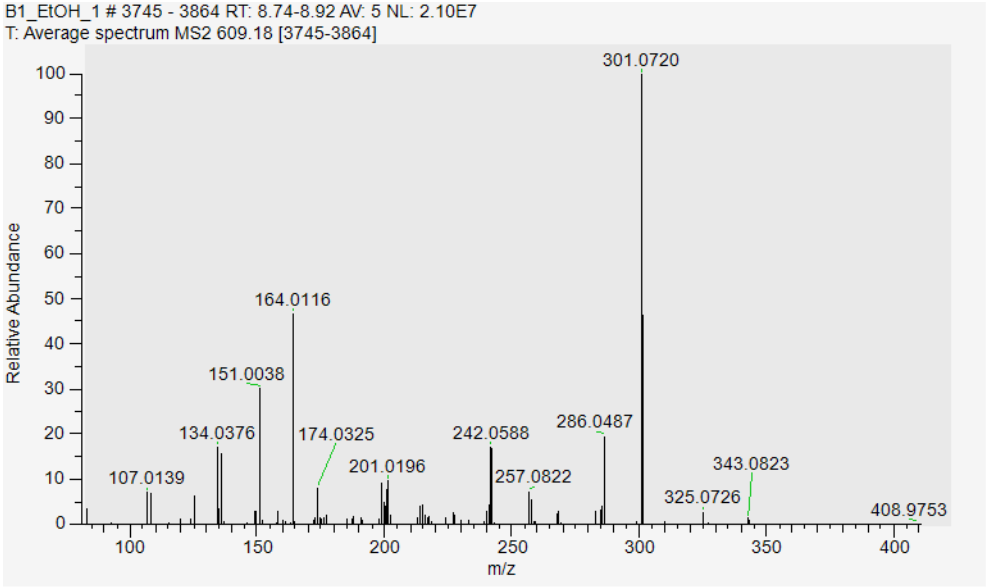

Figure SI 21: *MS² spectrum of hesperidin (precursor m/z 609.18). The spectrum shows characteristic losses of glucose and rhamnose, resulting in a prominent fragment at m/z 301.0720, corresponding to the aglycone hesperetin.*